How emissions, climate, and land use change will impact mid-century air quality over the United States: A focus on effects at National Parks

M. Val Martin[1,2], C. L. Heald[3], J.-F. Lamarque[4], S. Tilmes[4], L. K. Emmons[4], and B. A. Schichtel[5,6]

[1]Atmospheric Science Department, Colorado State University, Fort Collins, CO, USA
[2]Chemical and Biological Engineering Department, The University of Sheffield, Sheffield, UK
[3]Department of Civil and Environmental Engineering, Massachusetts Institute of Technology, Cambridge, MA, USA
[4]National Center for Atmospheric Research, Boulder, CO
[5]National Park Service, Fort Collins, CO, USA
[6]Cooperative Institute for Research in the Atmosphere, Fort Collins, CO, USA

Correspondence to: Maria Val Martin (m.valmartin@sheffield.ac.uk)

Abstract. We use a global coupled chemistry-climate-land model (CESM) to assess the integrated effect of climate, emissions and land use changes on annual surface O_3 and $PM_{2.5}$ in the United States with a focus on National Parks (NPs) and wilderness areas, using the RCP4.5 and RCP8.5 projections. We show that, when stringent domestic emission controls are applied, air quality is
5   predicted to improve across the U.S., except surface O_3 over the western and central U.S. under RCP8.5 conditions, where rising background ozone counteracts domestic emissions reductions. Under the RCP4.5 scenario, surface O_3 is substantially reduced (about 5 ppb), with daily maximum 8-hour averages below the primary U.S. EPA NAAQS of 75 ppb (and even 65 ppb) in all the NPs. $PM_{2.5}$ is significantly reduced in both scenarios (4 $\mu g/m^3$; $\sim$ 50%), with levels below the annual
10 U.S. EPA NAAQS of 12 $\mu g/m^3$ across all the NPs; visibility is also improved (10–15 deciviews; >75 km in visibility range), although some western U.S. parks with Class I status (40–74% of total sites in the U.S.) are still above the 2050 planned target level to reach the goal of natural visibility conditions by 2064. We estimate that climate-driven increases in fire activity may dominate summertime $PM_{2.5}$ over the western U.S., potentially offsetting the large $PM_{2.5}$ reductions from domestic
15 emission controls, and keeping visibility at present-day levels in many parks. Our study indicates that anthropogenic emission patterns will be important for air quality in 2050. However, climate and land use changes alone may lead to a substantial increase in surface O_3 (2–3 ppb) with important consequences for O_3 air quality and ecosystem degradation at the U.S. NPs. Our study illustrates the need to consider the effects of changes in climate, vegetation, and fires in future air quality
20 management and planning and emission policy making.

1 Introduction

Air pollution, such as surface ozone (O_3) and fine particulate matter (with diameter<2.5 μm; $PM_{2.5}$), has evolved in both urban and rural regions around the world over the last centuries. Air pollution changes have resulted in part from direct changes in natural and anthropogenic emissions and in part from indirect changes associated with climate and land use (Jacob and Winner, 2009; Arneth et al., 2010; Fiore et al., 2012). A changing climate is projected to significantly modify both natural and anthropogenic emissions and the atmospheric processes that govern air pollution transport, transformation, and deposition. For example, a warming climate is expected to increase wildfires and associated emissions of trace gases and particulate matter (Spracklen et al., 2009; Yue et al., 2013), cause a general increase in biogenic emissions (Heald et al., 2008), and increase emissions of O_3 and aerosol precursors, such as nitrogen oxides (NO_x) and ammonia (NH_3), from soil and agricultural activities. Anthropogenic emissions are likely to change in response to economic, climatic, and political pressures and policies (IPCC, 2013). In addition, a changing climate is likely to alter precipitation and cloud patterns and synoptic-scale transport processes (Jacob and Winner, 2009). At the same time, changes in land cover and land use will influence the deposition of pollution, as well as the emission of O_3 and aerosol precursors (Ganzeveld et al., 2010; Wu et al., 2012). For example, deforestation decreases turbulent exchange and foliar uptake, prompting a rise in air pollutants. These effects may drive significant local increases or decreases in air pollution.

National Parks (NPs) and wilderness areas in the United States (U.S.) are visited by millions of people every year to enjoy pristine nature. Maintaining adequate air quality conditions in these areas is key to preserving natural ecosystems, preventing negative impacts on visitor and staff health, and maximizing the beauty of landscapes. Air quality management in these regions, including efforts to develop meaningful emissions control strategies, relies on assessment of the current as well as future contributions of natural and anthropogenic sources to local air quality.

Two recent literature reviews (Jacob and Winner, 2009; Fiore et al., 2012) indicate that climate change alone will increase summertime surface ozone in polluted areas by 1–10 ppb. Pfister et al. (2014) predict an increase of about 5 ppb over the Rocky Mountain region during the summer in a future climate, with important implications for the U.S. National Park Service air quality management. Surface O_3 is toxic to humans and thus poses a threat to visitor and park staff health. In addition, accumulated exposure to elevated levels of O_3 can damage vegetation (eg Reich and Amundson, 1985; Schaub et al., 2005). Ozone levels have been shown to cause significant yield reduction in a number of major crops on a global scale (eg Avnery et al., 2011; Ghude et al., 2014), and in combination with warming may reduce global crop production by up to 15% in 2050 (Tai et al., 2014), leading to substantial economic losses and potentially worsening global malnutrition. Studies have also reported many other negative impacts on ecosystems, such as reductions in tree and seedling growth, decreases in photosynthetic rates, and visible foliar injuries on multiple plant species, including broadleaf deciduous forest in the northeastern U.S. and needleleaf evergreen forest in the

western U.S. (eg Arbaugh et al., 1998; Schaub et al., 2005). In addition, rising O_3 levels may substantially suppress the global land-carbon sink via its negative effect on photosynthesis, leading to a greater accumulation of carbon dioxide in the atmosphere (Sitch et al., 2007).

Atmospheric fine particles are also harmful to human and ecosystem health. Short-term exposure to $PM_{2.5}$ can lead to respiratory illness such as asthma; longer-term exposure may result in more severe cardiovascular and respiratory diseases as well as lung cancer, increasing the risk of premature mortality (eg Pope and Dockery, 2006). Fine particles and gases cause haze, which degrades visibility. Visibility is a protected attribute of some remote locations known as Class I areas, which includes many NPs and wilderness areas. The 1977 Clean Air Act set forth the goal to prevent future and remedy existing visibility impairment in Class I areas. In response, the U.S. Environmental Protection Agency (EPA) promulgated the Regional Haze Rule (RHR), which established the goal of returning visibility to natural conditions by the year 2064. Specifically, the RHR mandates that each state set "reasonable progress" goals to return visibility to natural conditions on the 20% haziest days by 2064, while preventing further degradation of visibility on the 20% clearest days (US EPA, 2003). Wild and prescribed fires are one of the primary contributors to air pollution, including haze-causing pollutants, in the western and southeastern U.S. (eg Val Martin et al., 2013). Previous studies project that increased fire activity over the western United States will nearly double carbonaceous aerosol by 2050, and produce a significant increase in annual mean $PM_{2.5}$ and haze (Spracklen et al., 2009; Yue et al., 2013).

In this study, we examine the integrated effect of climate change, anthropogenic emission changes, and land use change on air quality over the United States, with a particular focus on the U.S. National Parks. To our knowledge, this is the first time that the relative effect of these three factors has been considered for U.S. air quality projection. We use a global earth system model to estimate how surface O_3 and $PM_{2.5}$ are expected to change using two Representative Concentration Pathway (RCP) scenarios, represented in the IPCC (2013). We assess the changes in surface O_3 and $PM_{2.5}$ in 2050 relative to present-day levels and discuss the meteorological and chemical drivers behind these changes.

2 Modeling Analysis

2.1 Model description and future changes

To simulate the impact of future changes on the U.S. air quality, we use the Community Earth System Model (CESM) [http://www2.cesm.ucar.edu/]. CESM is a global model, which includes atmospheric, land, ocean and sea ice models that can be run in stand-alone or coupled configurations. We run CESM version 1.1.1 with online computed meteorology and prescribed sea-surface and sea-ice distributions, corresponding to previous fully-coupled simulations. Simulations are performed at

the horizontal resolution of 1.9° x 2.5°, and vertical resolution of 26 layers from the surface to about 4 hPa, with a time step of 30 minutes.

To simulate land processes, we use the Community Land Model (CLM) version 4 (Oleson et al.,
95 2010). CLM describes the physical, chemical, and biological processes of terrestrial ecosystems, including the hydrology and carbon cycling of the terrestrial biosphere.

For the atmospheric model, we use the Community Atmospheric Model (CAM) version 4 (Neale et al., 2013) fully coupled with an interactive gas-aerosol scheme (CAM-Chem) (Lamarque et al., 2012; Tilmes et al., 2014). The chemical mechanism includes full tropospheric O_3–NO_x–CO–VOC
100 and aerosol phase chemistry, based on the MOZART-4 chemical transport model (Emmons et al., 2010). Simulated aerosol mass classes include sulfate (SO_4), ammonium nitrate (NH_4NO_3), primary carbonaceous aerosols (black carbon, organic carbon), secondary organic aerosols (SOA), sea salt and dust. SO_4 is formed from the oxidation of SO_2 in the gas phase (by reaction with the hydroxyl radical) and in the aqueous phase (by reaction with ozone and hydrogen peroxide). NH_4NO_3 is
105 determined from NH_3 emissions and the parameterization of gas/aerosol partitioning by Metzger et al. (2002), which is based on the level of sulfate present. Black carbon (BC) and organic carbon (OC) aerosols are directly emitted in a combination of hydrophobic and hydrophilic forms (80% and 50% hydrophobic, respectively), and hydrophobic aerosol is converted to hydrophilic with a fixed 1.6 days e-folding time (Tie et al., 2005). Dust and sea salt are implemented following Mahowald et al.
110 (2006a, b), with improvements from Albani et al. (2014); the sources of these natural aerosols are derived based on the model calculated wind speed and surface conditions. SOA formation is linked to the gas-phase chemistry through the oxidation of isoprene, monoterpenes, alkenes and toluene as in Lack et al. (2004). Finally, dry deposition is represented by the multiple resistance approach of Wesely (1989), with some updates (Emmons et al., 2010; Lamarque et al., 2012; Val Martin
115 et al., 2014). The calculation of dry deposition velocities is performed in CLM and linked to land cover types. Therefore, dry deposition responds to changes in land cover and climate. In this work, we use the optimized dry deposition scheme described in Val Martin et al. (2014), in which the vegetation resistances are linked to the leaf area index (LAI). This optimized dry deposition scheme improves the simulation of O_3 dry deposition velocity, particularly over broadleaf forested regions,
120 and significantly reduces the well-known, long lasting summertime surface O_3 bias over eastern U.S. and Europe in CAM-Chem documented by Lamarque et al. (2012); we discuss this further in section 2.2.

We perform time-slice experiments for 2000 (present-day and baseline) and 2050 (future), under the RCP scenarios designed in support of the IPCC AR5. The RCPs include four scenarios, each
125 of which corresponds to a specific pathway towards reaching a 2100 target radiative forcing (RF) (i.e., 2.6, 4.5, 6.0 and 8.5 Wm^{-2}) associated with greenhouse gases: RCP2.6, RCP4.5, RCP6.0 and RCP8.5, respectively. The RCP2.6 assumes a peak forcing (3.0 Wm^{-2}) in the early 21st century and a decline out to 2100, the RCP4.5 and RCP6.0 scenarios assume RF stabilization after 2100, and the

RCP8.5 scenario assumes continuing growth in RF after 2100 (Moss et al., 2011). In this work, we

130 select the RCP4.5 and RCP8.5 scenarios to bracket our results, i.e., we use a stabilization scenario (RCP4.5) and the largest forcing scenario (RCP8.5). Table 1 summarizes the main climate input data for 2000 and 2050. We apply monthly mean time varying sea-surface temperatures and sea-ice distributions generated by the Community Climate System Model, version 4 for the Coupled Model Intercomparison Project Phase 5 (Meehl et al., 2012). Our simulations also consider time varying,

135 zonally averaged greenhouse gas distributions for CO_2, CH_4, N_2O and halogens, and future changes in stratospheric ozone levels.

Table 2 summarizes the main anthropogenic emissions for short-lived air pollutants and biogenic emissions projected over the United States. We divide the emissions for eastern and western U.S. because of the different emission patterns. Emissions of NO_x, NH_3, CO, non-methane volatile organic

140 compounds (VOCs), SO_2 and carbonaceous aerosols for anthropogenic activities and biomass burning are provided in 2000 by Lamarque et al. (2010) and in 2050 by the RCP database (van Vuuren et al., 2011, and references therein). Biomass burning emissions vary among the RCPs and in time, following changes in land cover and land use; however, they do not respond to changes in climate. Biogenic VOCs (e.g., isoprene and monoterpenes) are computed within CLM using the Model of

145 Emissions of Gases and Aerosols from Nature (MEGAN2.1) algorithms (Guenther et al., 2012), and are allowed to respond interactively to temperature, light, soil moisture, leaf age, CO_2 concentrations and vegetation density (Heald et al., 2008). In this work, we do not include the effect of CO_2, which suppresses isoprene production at elevated levels (eg Heald et al., 2008); we acknowledge that this is a limitation which will lead to a slight overestimate in isoprene emissions in 2050 because the

150 CO_2 inhibition would suppress about 10% the isoprene emission efficiency. Both dust and seasalt are also emitted interactively in CESM (Mahowald et al., 2006a, b; Albani et al., 2014). Lightning NO_x emissions are also calculated interactively in the model, as described in Lamarque et al. (2012). These emissions respond to climate and cannot be modified in the time-slice experiments. However, they are expected to have a very small impact on the overall surface ozone concentrations (Kaynak

155 et al., 2008). The global annual lightning emissions change from 4.2 Tg N yr^{-1} in 2000 to 4.4 and 4.8 Tg N yr^{-1} in 2050 for the RCP4.5 and RCP8.5 scenarios, respectively. Other natural emissions of O_3 and aerosols precursors (e.g., volcanoes, ocean and soil) may have some impact on surface O_3 and $PM_{2.5}$ on a regional scale over the United States. However, given the large uncertainties on how these emissions might vary in the future, we keep them constant at year 2000 levels.

160 In addition to climate forcing and emission changes, we include changes in land use induced by human activities in our simulations (Hurtt et al., 2011). We show projected 2050-2000 changes in crops, grasslands and trees over the U.S. for the RCP4.5 and RCP8.5 scenarios in Figure 1 as an example. The RCP4.5 scenario predicts an expansion of forested area, in particular over the eastern U.S. (10%) as a result of mitigation strategies for carbon emission reductions and a decline in agri-

165 cultural land (8%) due to this afforestation. Conversely, the RCP8.5 scenario predicts an important

5

increase in agricultural land (up to 5% in eastern U.S.) resulting from increasing population as well as grasslands (∼10%) and a decline in forest cover (2%).

For this study, we perform nine simulations: one simulation for present-day and four for each future scenario (Table 3). For the four simulations in the future, we modify one forcing at a time, and name these simulations after their future conditions, i.e., climate alone ("2050 Climate"), anthropogenic emissions including biomass burning emissions and methane levels ("2050 Emissions"), land cover and land use changes including climate-driven biogenic emissions ("2050 Land Use") and the combined effects of all the individual forcings ("2050 Total Change"). In the "2050 Land Use" simulation, climate-driven biogenic emissions are pre-calculated using the 2050 RCP4.5 and RCP8.5 climate projections. Each model simulation is initialized with a 1-year spin-up run. Following initialization, present-day and future "snapshot" forcing simulations are run for 9 years. We then average the results, and use all years to evaluate interannual variability and ultimately define statistical significance. We replicate these simulations for the RCP4.5 and RCP8.5 scenarios.

2.2 Model evaluation

The CESM simulations driven by online and offline meteorology have been extensively evaluated by comparison with satellite, sonde, aircraft and ground observations of key pollutants on a global scale (Lamarque et al., 2012). Here we focus our evaluation on annual $PM_{2.5}$ and O_3 over the United States and use long-term means from the Interagency Monitoring of Protected Visual Environments (IMPROVE) and the Clean Air Status and Trends Network (CASTNet) datasets. Both networks monitor air quality in rural areas at the surface all year round. We calculate long-term means from observations in 90 sites for CASTNet (1995–2005), and 194 sites for IMPROVE (1998–2010). Figure 2 compares observed and simulated surface O_3 and $PM_{2.5}$. For O_3, we use the metric for the U.S. EPA air quality standard of daily maximum 8-hour average (MDA-8); for $PM_{2.5}$, we focus on the annual average and determine $PM_{2.5}$ fine mass as the sum of SO_4, NH_4NO_3, organic aerosol (OA), BC, fine dust and seasalt. We compute OA assuming an average molecular weight of 2.0 per carbon weight for organic carbon (Malm and Hand, 2007). Organic carbon includes SOA. We summarize the comparison between the model and observations using the squared-correlation coefficient (r^2) and the normalized mean bias (NMB) (Figure 2c-d). In Figure 2c, we divide the O_3 comparison into eastern and western U.S. because of the different chemical regimes (eg Murazaki and Hess, 2006; Lamarque et al., 2012). For O_3, we find that simulated surface concentrations show good agreement with the mean observations over the western U.S. (r^2=0.77; NMB=4%), but slightly overestimate O_3 (r^2=0.47; NMB=16%) over the eastern United States. This annual overestimation is due to a positive bias in summertime O_3 (about 10 ppb), which is a well-known issue and has been previously documented in CESM (Lamarque et al., 2012) as well as other global and regional models (eg Murazaki and Hess, 2006; Fiore et al., 2009; Lapina et al., 2014). Using the optimized dry deposition scheme

(section 2.1), we significantly improve the simulation of summertime surface O_3, which has a 30 ppb bias (NMB=60%) over eastern U.S. in the standard dry deposition scheme (Val Martin et al., 2014).

We also evaluate the secondary metric W126 established to protect ecosystems and crops. The W126 is a biologically based index that estimates a cumulative ozone exposure over a 3-month growing season and applies sigmoidal weighting to hourly ozone concentrations (eg Lefohn et al., 1988; Lapina et al., 2014). The spatial distribution of W126 (not shown) is similar to the daily MDA-8 O_3 (Figure 2a), but exhibits larger values over regions of low and high ozone more emphasized due to the sigmoidal weighting of the W126 function as discussed in Lapina et al. (2014). We find that the model captures the spatial distribution of W126 across the US (r^2=0.70). However, the model tends to overestimate the magnitude by a factor of 3, in particular over the eastern United States. In previous studies, the lower performance of model simulations of W126 compared to those of daily MDA-8 O_3 has been attributed to the unbalanced sensitivity to model errors at the high end of the ozone concentration range (eg Tong et al., 2009; Hollaway et al., 2012; Lapina et al., 2014). For example, Lapina et al. (2014) report an overestimation of a factor varying between 2 and 4 over the United States in three chemical transport models.

For $PM_{2.5}$, we find that annual levels are well represented by CESM (r^2=0.70 and NMB=12%; Figure 2d). We further compare the simulated speciated $PM_{2.5}$ with observations in Figure 3. In our simulations, SO_4 and NH_4NO_3 are overestimated, whereas OA is underestimated. BC, dust and seasalt concentrations show good agreement with the mean observations, although with some scatter in the relationship (r^2 <0.40; not shown). These results are consistent with previous comparisons over the U.S. (Lamarque et al., 2012; Albani et al., 2014).

It is important to note that in our analysis we mainly concentrate in differences between present-day and future simulations, minimizing the impact of model biases.

2.3   Studied locations

We focus our analysis on the National Parks and wilderness areas located in the continental United States as shown in Figure 4. We consider the 352 units designated by the U.S. National Park System in the lower 48 states, of which 46 are classified as protected parks and the remaining as monuments, reserves, historical parks and sites and recreational areas. Additionally, we include 109 Class I areas in the lower 48 states that are not classified as National Park units, but in which air quality is also given special protection. In this work, we present results clustering the NPs and wilderness areas in six climatic regions (ie., Northeast, Southeast, Midsouth, Southwest, West and Great Plains) (Hand et al., 2012). We define these regions and highlight the protected parks in Figure 4.

3 Future changes in meteorological and chemical drivers

Climate and land cover and land use changes affect air pollution through changes in chemistry, transport, removal and natural emissions (eg Heald et al., 2008; Tai et al., 2012; Fiore et al., 2012). We examine here how some meteorological and chemical drivers are predicted to change in the future. Figure 5 shows present-day conditions and 2050-2000 changes in surface temperature, precipitation, boundary layer (BL) depth, isoprene emissions and O_3 dry deposition velocity. We only show changes predicted by the RCP4.5 scenario since the RCP4.5 and RCP8.5 scenarios have similar climates, but the RCP4.5 scenario has a more pronounced increase in isoprene emissions due to land use and climate change. Ozone deposition velocities also differ between the RCP4.5 and RCP8.5 simulations due to differences in projected land use change (Figure 1). To evaluate the statistical significance of our results, we use the Student-t test for a 95% confidence level and highlight the regions which are significant. Previous studies have investigated in detail the sensitivity of surface O_3 (eg Murazaki and Hess, 2006; Leung and Gustafson, 2005) and $PM_{2.5}$ (eg Tai et al., 2012; Leibensperger et al., 2012) to numerous climatic variables. In this work, we do not intend to assess the impact that each climatic variable has on the total change in $PM_{2.5}$ and surface O_3. Instead, we provide here an overview on how these drivers may impact our simulated O_3 and $PM_{2.5}$.

Surface temperature is predicted to increase by an average of 1.7°C across the U.S. due to the rising greenhouse gases in the RCP 4.5 scenario (Figure 5a). The extent of this increase varies across the U.S., with a maximum increase of 4°C observed over the central United States. The RCP8.5 scenario predicts a similar increase to the RCP4.5 scenario: 2.0°C. We find that the 9-year simulations generate robust increases in surface temperature changes across most of the continental United States. Previous studies have reported similar results with distributions and magnitudes differing slightly depending on the model, resolution and the climate scenario considered (eg Murazaki and Hess, 2006; Kelly et al., 2012; Pfister et al., 2014). It is known that high ozone levels correlate well with temperature in many polluted regions due to the connection between temperature to stagnation conditions, enhanced photochemistry and biogenic and wildfire emissions (Fiore et al., 2012, and references therein). $PM_{2.5}$ is also affected by many of the same meteorological processes as surface O_3, although the relationship is more complex and the sign of the effect can be positive or negative because of the different sensitivities of the $PM_{2.5}$ chemical species (eg Tai et al., 2012). Thus, our simulated increase in temperature will intensify surface O_3 and most probably $PM_{2.5}$ pollution over the United States.

Air quality is also sensitive to precipitation and cloud cover. For example, $PM_{2.5}$ is expected to decrease in regions with increased precipitation (eg Pye et al., 2009; Racherla and Adams, 2008). In our simulations, precipitation decreases over most of the continental U.S. (30%), with some small increases over some regions in the northwestern U.S. (8%) (Figure 5b). However, not all of the changes in precipitation are significant and the absolute changes are generally small (<1 mm/day) despite the large percentage change. We find similar pattern in the cloud cover (not shown). A decrease in

270   cloudiness is associated with an increase in solar radiation, which favors surface O_3 production in

our simulations.

    An important meteorological process for diluting and transporting air pollutant is mixing within

the boundary layer. In our simulations, the boundary layer depth across the U.S. is predicted to

generally increase, with the largest increase over in central U.S. (>100 m; about 20%) (Figure 5c).

275   Increases in BL depth favors ventilation and reduces pollutant accumulation. In our simulations, we

notice that BL depth increases (i.e., favoring low $PM_{2.5}$ and O_3 concentrations) and precipitation

(and cloud cover) decreases (i.e., favoring high $PM_{2.5}$ and O_3 concentrations) are generally co-

located. These two processes have opposite effects on air quality and this highlights the challenges

in predicting possible air quality impacts resulting from climate change.

280   Higher temperature and solar radiation will also affect biogenic emissions, which in turn will in-

fluence $PM_{2.5}$ and surface O_3. Biogenic emissions will also depend on land use changes. In 2050,

isoprene emissions are predicted to increase from 28 to 43 Tg C (about 53%) in the U.S. (Table 2),

with 10% of this increase driven by land use changes. This effect is more significant in the south-

eastern U.S. (about 25%) due to afforestation (Figure 5d). The RCP8.5 scenario also predicts an

285   increase in biogenic emissions, but with a lower influence from land use and climate changes (33%;

not shown). We note that our isoprene emissions are slightly overestimated as we neglect the effect

of CO_2 inhibition, explained in Section 2.1. Increased emissions of biogenic volatile organic com-

pounds (e.g. isoprene) will increase $PM_{2.5}$ through SOA formation (Heald et al., 2008). For ozone,

the impact of changing biogenic emissions depends critically on the fate of isoprene nitrates, i.e.,

290   whether isoprene nitrate is a terminal or temporal sink of NO_x (eg Horowitz et al., 2007; Wu et al.,

2012). In our model, isoprene nitrate recycles 40% of NO_x (Horowitz et al., 2007). Therefore, in-

creases in biogenic emissions tend to enhance surface O_3, regardless of the NO_x concentrations.

This O_3 response to NO_x with respect to changes in biogenic emissions is slightly different than

other models, where isoprene nitrates represent a terminal sink of NO_x. In those cases, increases

295   in isoprene emissions lead to increases or decreases in surface O_3 concentrations depending on the

availability of NO_x (eg Wu et al., 2012; Mao et al., 2013).

    Land use changes can also influence deposition processes. For example, large O_3 dry deposi-

tion velocities are associated with denser, broadleaf forests (i.e., with high LAI) and crops (eg We-

sely, 1989; Val Martin et al., 2014), whereas grasslands and needleleaf forests (i.e., with low LAI)

300   are characterized by low deposition velocities. In our simulations, the O_3 dry deposition velocity

generally shows a small decrease across the U.S. (0.2–1.0 cm/min; about 1–3%) (Figure 5e). The

RCP8.5 scenarios projects more variable, but even smaller changes in the O_3 dry deposition velocity

(<0.6%), associated with a less pronounced change in vegetation. Interestingly, in this study we find

a reduction in the annual O_3 dry deposition velocity due to the shift from croplands to grasslands

305   and forests. This result contrasts with previous studies that report decreased dry deposition velocities

in regions with increased agricultural land (Ganzeveld et al., 2010; Wu et al., 2012). However, these

9

studies focus on either summertime changes when broadleaf forests have a larger dry deposition velocity than crops (Wu et al., 2012) or use a different dry deposition parameterization (Ganzeveld et al., 2010). We note that the resulting changes in the deposition velocities in our model are not
310 significant at the 95% confidence level and these two previous studies do not evaluate the statistical significance of their results. Nonetheless, this comparison underlines the important effect that land-use change assumptions may have on the projections of future air quality.

4 Future PM$_{2.5}$ air quality

In this section, we first examine how total and speciated PM$_{2.5}$ are predicted to change in the future
315 due to climate, emissions and land use changes. We then discuss the impacts of future climate-driven wildfire activity in PM$_{2.5}$ and haze.

4.1 Regional annual changes in PM$_{2.5}$

Figure 6 shows changes in annual surface PM$_{2.5}$ concentrations following the RCP4.5 and RCP8.5 scenarios over the continental United States. The projected changes in 2050 from the combined
320 effects and the individual effects of emissions, climate and land use change are also shown. The "emissions" simulation takes into account changes in anthropogenic and biomass burning emissions and methane levels; the "land use" simulation is associated with changes in climate-driven biogenic emissions and land cover. We also indicate the regions with confidence levels higher than 95% from the Student-t test; we find that the 9-year simulations generate robust results across most of the
325 continental U.S. for the simulations with the combined effects and emissions alone.

The combined effects of changing climate, land use, and emissions lead to a strong decrease in PM$_{2.5}$ concentrations across the continental U.S. (Figure 6a), with an average projected decrease of about 4 μg/m^3 ($\sim$50%) for both the RCP4.5 and RCP8.5 scenarios. The absolute decrease is stronger in the eastern than in the western U.S., about 4 μg/m^3 versus 2 μg/m^3, because the eastern
330 U.S. is characterized by larger PM$_{2.5}$ concentrations (Figure 2b). Projected changes in U.S. PM$_{2.5}$ for 2050 largely reflect changes in anthropogenic emissions, which drive the majority ($>$95%) of this decrease all over the United States. The contribution of climate and land use changes, although minor and rather insignificant in most of the U.S., may counteract the benefits of emissions reductions in some regions (Figure 6b). For example, the RCP4.5 scenario projects a 47% total average decrease
335 in PM$_{2.5}$ in the Southwest region, with about 52% drop due to emission reductions, but a counter veiling increase of 5% and 0.1% from climate and land use, respectively. In many regions the impact of climate or land use change is not significant compared to climate variability when averaging over 9 years.

To examine in more detail future changes in PM$_{2.5}$ we show changes in speciated PM$_{2.5}$ in Fig-
340 ure 7. We find that the decrease in PM$_{2.5}$ concentrations is mainly driven by decreases in SO$_4$ and, to

10

a lesser extent, in NH_4NO_3 and BC. Under the RCP4.5 and RCP8.5 scenarios, anthropogenic SO_2 emissions are projected to decrease substantially in the western and the eastern U.S. compared to present-day (84% and 89% in RCP4.5 and 69% and 90% in RCP8.5, respectively; Table 2). Large decreases in NO_x emissions are also projected (75% and 78% in RCP4.5 and 50% and 72% in RCP8.5), whereas NH_3 emissions increase (33% and 25% in RCP4.5 and 59% and 44% in RCP8.5). The largest significant change in $PM_{2.5}$ is projected with the RCP8.5 scenario over the Northeast region, with a decrease of 90% in BC, 79% in SO_4 and 46% in NH_4NO_3. Organic aerosol increases slightly, in particular over the Northeast, Southeast and West regions. This increase does not offset the decreases in the other species, yet it can be important in some regions. Over the Southeast, the RCP4.5 and RCP8.5 scenarios project similar decreases in SO_4, NH_4NO_3 and BC. However, $PM_{2.5}$ concentrations are predicted to be lower in the RCP8.5 than in the RCP4.5 scenario because of the relative importance of OA in the total $PM_{2.5}$ loading. Higher OA concentrations in the RCP4.5 scenarios result from higher VOC emissions (Table 2) associated with reforestation and climate change, as discussed in section 3.

Our results are consistent with previous studies, which have shown the small impact of climate change on $PM_{2.5}$ levels and the significant contribution from projected emissions reductions (eg Tagaris et al., 2007; Pye et al., 2009; Lam et al., 2011; Kelly et al., 2012). Comparing $PM_{2.5}$ projections from different studies is not straightforward due to variations in the study region, reported $PM_{2.5}$ metrics and use of different climate and emissions (Fiore et al., 2012). A decrease of about 2 $\mu g/m^3$ (25%) over the U.S. was projected for the SRES A1B scenario by Tagaris et al. (2007) for the combined effect of climate and emissions, with the bulk of this decrease resulting from sulfate, nitrate and ammonium reductions. Using the same scenario, Lam et al. (2011) found a similar decrease (4–5 $\mu g/m^3$), with 90% of the reduction due to emission reductions. Most recently, Kelly et al. (2012) reported summertime regional decreases of more than 3 $\mu g/m^3$ over the U.S., with the SRES A2 climate and RCP6.0 emission scenarios.

We summarize the simulated $PM_{2.5}$ changes over the U.S. NP and wilderness areas in Table 4. We show results for the 46 protected National Parks located in the continental United States. We find that the RCP4.5 and RCP8.5 scenarios predict a significant reduction of $PM_{2.5}$ levels across the protected NPs, with the exception of the Crater Lake and Lassen Volcanic NPs. In these two NPs, the RCP8.5 scenario projects a slight increase in annual $PM_{2.5}$, but concentrations are predicted to remain below 12 $\mu g/m^3$, the primary annual U.S. National Ambient Air Quality Standards (NAAQS) for $PM_{2.5}$. In the Joshua Tree NP, both RCP scenarios predict a significant improvement of $PM_{2.5}$ air quality, but with an annual average above 12 $\mu g/m^3$ due to the dominance of natural dust in this region.

It is important to note that changes in the frequency and magnitude of the fire resulting from climate change are not included in this analysis, and this effect may have an important impact on the $PM_{2.5}$ levels associated with climate change, as discussed in the following section.

11

4.2 Effects of increased fire activity on summertime PM$_{2.5}$

Climate-driven changes in fire emissions can be an important factor controlling PM$_{2.5}$ concentrations (Spracklen et al., 2009; Yue et al., 2013). Yue et al. (2013), use results from 15 climate models following the SRES A1B scenario and a fire prediction model of area burned to predict increases of 63–169% in area burned over the western U.S. in 2050, which leads to about 150–170% increases in OC and BC fire emissions. The RCP4.5 scenario predicts an increase of about 60% in OC fire emissions over the western U.S., whereas the RCP8.5 projects a marginal decrease of 0.3%. These two RCP scenarios clearly underestimate the average increase in carbonaceous aerosol fire emissions associated with climate feedbacks as projected by Yue et al. (2013).

To assess the importance of climate-driven fire emissions on future PM$_{2.5}$, we perform an additional simulation (not shown in Table 3), where we increase the RCP fire emissions over the U.S. in order to match Yue et al. (2013)'s projection. In doing so, we keep the spatial distribution of fire as described by the RCP scenarios and apply a homogeneous increase on a monthly basis. We scale the RCP fire emissions over the U.S. and Canada, with the exception of the eastern U.S., where fire activity is not predicted to significantly increase in the future due to climate (Scholze et al., 2006; Moritz et al., 2012).

Figure 8 shows the effect of climate-driven fire emissions on summertime PM$_{2.5}$. We focus on the summer here which is the peak fire season in the United States. We compare the PM$_{2.5}$ levels predicted by the RCP scenarios in 2050 to those when climate-driven fire activity is included, and only show those climatic regions where PM$_{2.5}$ is affected by fire, i.e., West, Great Plains, Southwest and Northeast. PM$_{2.5}$ concentrations in these regions increase significantly as a result of increased fire activity. These increases are most prominent over the West and Great Plain regions, in which fire-driven PM$_{2.5}$ may potentially offset anticipated reductions in anthropogenic emissions. For example, over the West region we estimate that fire activity may increase future summertime PM$_{2.5}$ from 3.2 μg/m^3 to 5.2 μg/m^3 (63%) in the RCP8.5 scenario and from 4.5 to 5.6 μg/m^3 (22%) in the RCP4.5 scenario. The concentration of organic aerosol nearly doubles in both scenarios, and this dominates the total change in PM$_{2.5}$. It is important to note that our fire OA may be underestimated as we do not include secondary production of OA from fire emissions. Increased fire activity may also affect PM$_{2.5}$ further downwind from the fires. We estimate that summertime PM$_{2.5}$ may increase up to 4–10% in the Northeast region due to smoke transported from fires in the western U.S. and the boreal region.

Therefore, changes in summertime PM$_{2.5}$ concentrations may be dominated by changes in fire activity in most of the western U.S. in a future climate. This same fire pollution may significantly impair visibility over this region, as well as hundreds of kilometers downwind from the fire sources.

4.3 Effects on future visibility

We evaluate the effects of future changes in visibility in the U.S. NP and wilderness areas across the continental U.S. by examining changes in the haze index (HI) and visibility range. We calculate the HI based on the definition of the US EPA (2003) and the visibility range as in Pitchford and Malm (1994) using the results of the daily averages of $PM_{2.5}$ chemical species. Figure 9a shows changes in HI for the most polluted and the cleanest episodes (ie, worst and best days, respectively) predicted by the RCP4.5 and RCP8.5 scenarios. We define most polluted and cleanest episodes as those days characterized by aerosol levels with the 20% worst and best visibility, that is, with the HI above the 90th percentile or below the 10th percentile, respectively (US EPA, 2003). As an example, we show in Figure 9b the cumulative distribution function of daily HI over two protected national parks: Crater Lake and Acadia NP, located over the West and Northeast region, respectively. We also include the impact of fire pollution in this analysis and indicate the 2050 HI target required to reach natural background conditions by 2064 as mandated by the Regional Haze Rule.

Consistent with the $PM_{2.5}$ projections, we predict a significant visibility improvement in both polluted and background conditions over the continental United States. This improvement results mainly from the large reduction in anthropogenic emissions, with the strongest absolute reductions in areas with high $PM_{2.5}$ and high anthropogenic aerosol precursor emissions such as the Northeast region. In this region, our results show a reduction of up to 15 deciviews during cleanest days and up to 10 deciviews during most polluted events in both RCP scenarios, which corresponds to an increase of more than 75 km in visibility range.

The improvement in $PM_{2.5}$ air quality is reflected in the projected visibility over the U.S. National Parks and wilderness areas. For example, in Acadia NP, we find that both RCP scenarios predict HI level decreases of about 10 deciviews during the most polluted events, leading to an improvement in visibility range of more than 70 km. This NP is estimated to reach the 2050 target to restore natural visibility conditions by 2064, even during most polluted conditions. However, this is not the case for all the protected NPs and wilderness areas. Our results show that visibility in Crater Lake NP is estimated to improve by 2050, with moderate HI decreases ($\sim$ 4 deciviews) predicted by both RCP scenarios, and a general improvement of visibility range of 30–40 km. However, HI levels are predicted to remain higher than the 2050 target. This is also the case for other important NPs located in the western U.S. such as Yellowstone, Grand Canyon, and Mount Rainier NPs; about 40% and 74% of the total parks may not reach the 2050 target as predicted by the RCP4.5 and RCP8.5 scenarios, respectively.

Future regional visibility may also be impaired by fire pollution resulting from climate change. We find that fire pollution may maintain visibility levels at present-day conditions during the most polluted events in some NPs and wilderness areas (e.g. Crater Lake NP; Figure 9b) or may impede the attainment of the 2050 visibility target (e.g. Yellowstone NP; not shown). Our analysis shows little or no effect of fire in visibility impairment in NPs and wilderness areas located in the Northeast

13

and Southeast climatic regions (e.g., Acadia NP; Figure 9b). Yue et al. (2013) estimate that future

450   fire activity would lead to an average visibility decrease of 30 km in the 32 Federal Class I areas

located in Rocky Mountains Forest. Our predictions for the Rocky Mountain NP show more moder-

ate decreases in visibility (4–6 km; not shown). However, our work differs from Yue et al. (2013) in

both the model resolution (200 km versus 400 km) and the spatial distribution of the fire emissions.

5   Future changes in surface O_3

455   In this section, we first examine future projections on daily surface MDA-8 O_3 concentrations and

evaluate the contributing factors to this future change. We then discuss how future changes in surface

O_3 may impact ecosystems.

5.1   Predictions of daily O_3 concentrations

Figure 10 shows the 2050–2000 changes in annual mean surface O_3 concentrations predicted by the

460   RCP4.5 and RCP8.5 scenarios in the continental United States. As in the $PM_{2.5}$ analysis, we present

total changes in the simulated daily MDA-8 O_3 concentrations and show the individual perturbations

resulting from changing climate, land use, and emissions including methane concentrations (Fig-

ure 10a). We also highlight the regions with confidence levels higher than 95% from the Student-t

test.

465   The combined effects of changing emissions, climate and land use produce a strong decrease in

surface O_3 across the continental U.S. in the RCP4.5 scenario, with the strongest absolute reductions

(up to 10 ppb) over the eastern U.S. and California, regions with the highest O_3 concentrations (Fig-

ure 2a) and strongest anthropogenic precursors emissions reductions. The average MDA-8 over the

U.S. decreases from 52 ppb to 47 ppb from present to future days. However, the RCP8.5 scenario

470   predicts important increases over the Great Plain region (about 5 ppb) and marginal decreases (about

2 ppb) over the eastern U.S. and California. During summertime (not shown), these changes are sim-

ilar but more pronounced because O_3 concentrations are the highest during this season: summertime

MDA-8 decreases from 62 to 51 ppb in the RCP4.5 scenario and increases (about 6 ppb) over the

Great Plain region and decreases (up to 15 ppb) over the eastern U.S. and California in the RCP8.5

475   scenario.

The RCP4.5 and RCP8.5 scenarios project strong and similar decreases in domestic O_3 precursor

emissions (Table 2), however global CH_4 concentrations are 50% larger in RCP8.5 compared to

RCP4.5 (2740 versus 1838 ppb; Table 1). Rising surface O_3 levels over central U.S. in the RCP8.5

scenario are therefore the result of elevated background O_3 due to rising CH_4 levels in combination

480   with climate and land use changes. These individual effects can be clearly seen in Figure 10b, which

shows that climate and land use changes completely offset the emission reductions over the West

and Midsouth regions in the RCP8.5 scenario. For example, in the West region, the RCP8.5 scenario

14

predicts an overall increase of 3% in surface O_3 ($\sim$3 ppb), in which the contribution from emission reductions (-2%) is counterbalanced by climate (+3%) and land (+2%) changes.

485 The impact of the rising background O_3 in the RCP8.5 scenario can also be seen on the surface O_3 concentrations over the ocean. Similar to previous studies (eg Wu et al., 2008; Fiore et al., 2012), the RCP4.5 scenario projects a decrease in O_3 levels (up to 5 ppb) over the Pacific and Atlantic oceans in a changing climate due to the decrease of O_3 lifetime associated with higher water vapor. The shorter lifetime of PAN in a future climate may also contribute to the decrease of O_3 levels over

490 remote areas (eg Wu et al., 2008; Doherty et al., 2013). By contrast, the RCP8.5 scenario projects an increase in surface O_3 (up to 8 ppb) due to the rising background over these remote regions.

 Climate and land use changes alone are also expected to significantly impact future O_3 air quality. When only climate change is considered and the emissions of ozone precursors are held at present-day levels ("Climate" simulation), simulated surface O_3 increases by 1 and 2 ppb across the U.S. in

495 the RCP4.5 and RCP8.5 scenarios respectively, with the largest absolute changes over the eastern U.S. (up to 3 and 5 ppb, respectively). Note that this "climate penalty" does not include the effect of changing biogenic emissions, which is incorporated in the land use change simulations. However, Tai et al. (2013) show that the offsetting effects of climate and CO_2 inhibition substantially reduce the role of isoprene emission changes in the climate penalty. Thus, the climate effect shown here

500 may be a good proxy for the climate penalty and is comparable to values shown by Tai et al. (2013). In the land use change simulation, surface O_3 increases by 2 ppb in both scenarios, with the largest increases over the central U.S. (up to 8 and 4 ppb, respectively). Increases in surface O_3 result mainly from climate-driven increases in biogenic VOCs and, to a lesser extent, from a decrease in dry deposition velocity due to the shift from croplands to grasslands projected in both scenarios

505 over this region. It is clear that our land use impacts may be slightly overestimated because we do not include the effect of CO_2 inhibition in our isoprene emissions, as discussed in Sect. 2.1. However, this does not change the positive effect that changes in land use cover have on surface ozone concentrations.

 Our projected change in surface O_3 is more moderate than that reported in previous studies (eg

510 Tagaris et al., 2007; Nolte et al., 2008; Kelly et al., 2012; Pfister et al., 2014). However, these studies do not account for changes in land cover, which our work indicates can be regionally quite substantial. Furthermore, Parrish et al. (2014) show that models (including CAM-Chem) typically underestimate the O_3 response to emissions changes; thus, our sensitivities likely represent a lower limit, and even larger emission-driven changes in O_3 surface concentrations may be anticipated in

515 coming decades. Finally, it is important to note that the effects of emissions, climate and land use need to be considered together when studying changes in surface O_3 since these individual forcings interact in a strongly non-linear fashion. For example, surface O_3 changes in the RCP8.5 scenario are 15% larger in the linear sum of the individual forcings than in the combined effects.

Figure 11 shows the impact of these changes on surface O_3 over the U.S. National Parks and wilderness areas. Under RCP8.5 conditions, we find an improvement of surface O_3 air quality for most polluted days (ie. high tail of the distribution is lower than present-day), except in the Great Plains region, and a deterioration in the background O_3 (i.e., the low tail of the distribution is higher than present-day) all across the United States. These results are due to increases in CH_4 emissions in combination with the effects of climate and land use changes as discussed above. However, under RCP4.5 conditions, there is a clear general improvement of surface O_3 air quality across the U.S., with the exception of increasing background O_3 in the Northeast, Southeast and Midsouth regions. Furthermore, as discussed in Pfister et al. (2014), background O_3 at high elevations may be affected by long-range transport of pollution and stratospheric intrusions (eg Eyring et al., 2010; Lin et al., 2012). Both processes are taken into account in our simulations (but not disaggregated), and are expected to change in the future due to decreasing NO_x emissions in Asia (van Vuuren et al., 2011) and the recovery of the stratosphere O_3 layer (Eyring et al., 2010; Kawase et al., 2011).

In all of the U.S. protected NPs and wilderness areas (Table 4), surface O_3 levels are predicted to improve under the RCP4.5 scenario. We estimate that annual concentrations are projected to be below the current primary EPA NAAQS of 75 ppb to protect public health, and even below a more restrictive potential future standard of 65 ppb. In contrast, under RCP8.5 conditions, numerous parks and wilderness areas are predicted to have poorer O_3 air quality. For example, 34 out of the 46 protected NPs in the lower 48 states may encounter surface O_3 increases with respect to present-day levels (e.g., Glacier and Yellowstone NPs), although projected concentrations are below 65 ppb. However, during the summer, when O_3 concentrations are higher, 16 out of 46 NPs are predicted to have summertime surface O_3 levels above 65 ppb (e.g., Rocky Mountain and Yosemite NPs) (not shown).

5.2 Effects on future ecosystem O_3 damage

To investigate the effect of projected changes in surface O_3 levels in the U.S. NPs and wilderness areas, we use the secondary metric W126 established to protect ecosystems and crops. Figure 12 presents average W126 over the U.S. NPs and wilderness areas divided in the 6 climatic regions for present-day and future. We focus on summertime W126 as the summer season is the growing season for many ecosystems and show the 2050–2000 difference in W126 to minimize the influence of the positive bias in the simulated W126 index, as discussed in section 2.2.

Consistent with the daily O_3 pattern, the RCP4.5 and RCP8.5 scenarios project a decrease in the W126 index across the continental U.S., with the exception of the Great Plain region by the RCP8.5 scenario. The RCP4.5 scenario projects a general decline in W126: from strong decreases (-39 ppm-hr) in the North East to more moderate decreases (-8 ppm-hr) in the Great Plains. Under RCP8.5 conditions, the changes in W126 are more modest, with decreases of -37 ppm-hr in the North East and increases of $+7$ ppm-hr in the Great Plains. Despite the general decrease in daily surface O_3

16

555 predicted by both scenarios from strong emission reductions, our results suggest that the decreases in the W126 index may not be sufficient to keep W126 above the suggested range for a secondary standard (7–15 ppm-hr) to protect vegetation (not shown); however, this is difficult to quantitatively assess here given the current model bias.

The simulated W126 over the U.S. protected NPs is summarized in Table 4. Our study shows that
560 a number of protected NPs will experience W126 levels exceeding the secondary standard to protect vegetation. The RCP8.5 scenario projects that the majority of the protected parks will have an W126 index above the recommended limits, with 34 parks above 7 ppm-hours and 26 parks above 15 ppm-hours; projections from the RCP4.5 result in 26 and 6 parks, respectively. We note that our results indicate an upper limit on the impacts of surface O_3 concentrations on vegetation given the model
565 positive bias in the W126 index. Nonetheless, this study suggests that O_3 pollution may remain a threat to ecosystems in the U.S. NPs and wilderness areas despite the substantial general decrease in surface O_3 concentrations.

6 Conclusions

We have quantified for the first time changes in air quality between present and a 2050 future pe-
570 riod associated with changes in emissions, climate, and land use change over the United States. In particular, we focus on the implications of these projections for air quality in National Parks and wilderness areas.

We find that, if stringent domestic emission controls are applied in the future such as those projected by the RCP4.5 and RCP8.5 scenarios, air quality is predicted to improve significantly across
575 the U.S., except surface O_3 in the central U.S. under RCP8.5 conditions. We estimate that $PM_{2.5}$ concentrations in the majority of the U.S. NPs and wilderness areas will be substantially reduced, below the annual U.S. EPA NAAQS of 12 $\mu g/m^3$. In addition, visibility will be in general significantly improved. Over the eastern U.S., we estimate that most of the parks will reach the 2050 target to restore visibility to natural conditions by 2064, whereas some parks may not reach this tar-
580 get during most polluted episodes over the western U.S. (e.g., Yellowstone and Grand Canyon NP). This result suggests that, to obtain acceptable future visibility conditions over this region, the U.S. National Park Service may have to develop specific air quality management plans to include further mitigation strategies beyond those projected by the RCP scenarios.

Our analysis shows that climate-driven fires may dominate summertime $PM_{2.5}$ concentrations
585 in the future over the western U.S., potentially offsetting the large $PM_{2.5}$ reductions from anthropogenic emission controls. Future regional visibility is also estimated to be impaired by fire pollution, which may keep visibility at present-day levels during the most polluted episodes in many parks (e.g., Crater Lake NP). However, our analysis has important limitations. For example, it considers an average fire emission projection based on SRES A1B climate and applies this projection homoge-

17

590 neously to all the fire species on a monthly basis and with the spatial distribution formulated by the RCP fire emission database. More work is needed to directly couple climate-driven fire emissions, vegetation dynamics, and air quality.

We find that daily surface O_3 is projected to drop in all U.S. NPs and wilderness areas in the RCP4.5 scenario, with MDA-8 levels below the primary U.S. EPA NAAQS of 75 ppb to protect

595 human health, and even below 65 ppb, a level considered for future regulation. In contrast, our projections with the RCP8.5 scenario indicate that numerous parks in the western and central U.S. are predicted to have a poorer O_3 air quality, with MDA-8 above 65 ppb in some cases during the summer (e.g., Rocky Mountain and Yellowstone NP). In this case, the rising O_3 resulting from a growing O_3 background associated with increases in CH_4 levels ($\sim$1000 ppb) as well as climate and land

600 use changes exceeds the important surface O_3 reductions projected from anthropogenic emission controls. Furthermore, despite the substantial general decrease in surface O_3, our study suggests that the secondary standard W126 may remain above the recommended limits (7–15 ppm-hrs) to protect vegetation in many regions across the United States. Thus, future O_3 pollution may be a threat to the U.S. NP ecosystems. In the U.S., W126 levels are most sensitive to domestic anthropogenic NO_x

605 emissions (Lapina et al., 2014) and our results suggest that more restricted policies for NO_x control may be needed to preserve natural ecosystems in the U.S. NPs and wilderness areas.

Our results suggest that 2050 air quality in the U.S. will likely be dominated by anthropogenic emission trajectories. Changes in air quality driven by climate and land use are small over the 50-year time horizon studied here and they are not always significant. However, climate alone can lead to a

610 substantial increase in surface MDA-8 O_3 by 2050 over most of the U.S. with important implications for O_3 air quality and ecosystem health degradation at the U.S. National Parks. Projected changes in temperature, cloud cover, and biogenic emissions suggest that these drivers may exacerbate future O_3 pollution across the United States. Furthermore, land use change may have an important regional effect on surface O_3, due to changes in biogenic emissions and dry deposition. Our study suggests

615 that the effects of climate, vegetation, and fires are important in future air quality projections and these processes should be considered in air quality management and planning in the coming decades.

References

Albani, S., Mahowald, N. M., Perry, A. T., Scanza, R. A., Zender, C. S., Heavens, N. G., Maggi, V., Kok, J. F., and Otto-Bliesner, B. L.: Improved dust representation in the Community Atmosphere Model, Journal of Advances in Modeling Earth Systems, 06, n/a–n/a, doi:10.1002/2013MS000279, http://dx.doi.org/10.1002/2013MS000279, 2014.

Arbaugh, M. J., Miller, P. R., Carroll, J. J., Takemoto, B., and Procter, T.: Relationships of ozone exposure to pine injury in the Sierra Nevada and San Bernardino Mountains of California, {USA}, Environmental Pollution, 101, 291 – 301, doi:http://dx.doi.org/10.1016/S0269-7491(98)00027-X, http://www.sciencedirect.com/science/article/pii/S026974919800027X, 1998.

Arneth, A., Harrison, S. P., Zaehle, S., Tsigaridis, K., Menon, S., Bartlein, P. J., Feichter, J., Korhola, A., Kulmala, M., O'Donnell, D., Schurgers, G., Sorvari, S., and Vesala, T.: Terrestrial biogeochemical feedbacks in the climate system, Nature Geosci, 3, 525–532, http://dx.doi.org/10.1038/ngeo905, 2010.

Avnery, S., Mauzerall, D. L., Liu, J., and Horowitz, L. W.: Global crop yield reductions due to surface ozone exposure: 1. Year 2000 crop production losses and economic damage, Atmospheric Environment, 45, 2284 – 2296, doi:http://dx.doi.org/10.1016/j.atmosenv.2010.11.045, http://www.sciencedirect.com/science/article/pii/S1352231010010137, 2011.

Doherty, R. M., Wild, O., Shindell, D. T., Zeng, G., MacKenzie, I. A., Collins, W. J., Fiore, A. M., Stevenson, D. S., Dentener, F. J., Schultz, M. G., Hess, P., Derwent, R. G., and Keating, T. J.: Impacts of climate change on surface ozone and intercontinental ozone pollution: A multi-model study, Journal of Geophysical Research: Atmospheres, 118, 3744–3763, doi:10.1002/jgrd.50266, http://dx.doi.org/10.1002/jgrd.50266, 2013.

Emmons, L. K., Walters, S., Hess, P. G., Lamarque, J.-F., Pfister, G. G., Fillmore, D., Granier, C., Guenther, A., Kinnison, D., Laepple, T., Orlando, J., Tie, X., Tyndall, G., Wiedinmyer, C., Baughcum, S. L., and Kloster, S.: Description and evaluation of the Model for Ozone and Related chemical Tracers, version 4 (MOZART-4), Geosci. Model Dev., 3, 43–67, doi:10.5194/gmd-3-43-2010, http://www.geosci-model-dev.net/3/43/2010/, 2010.

Eyring, V., Cionni, I., Bodeker, G. E., Charlton-Perez, A. J., Kinnison, D. E., Scinocca, J. F., Waugh, D. W., Akiyoshi, H., Bekki, S., Chipperfield, M. P., Dameris, M., Dhomse, S., Frith, S. M., Garny, H., Gettelman, A., Kubin, A., Langematz, U., Mancini, E., Marchand, M., Nakamura, T., Oman, L. D., Pawson, S., Pitari, G., Plummer, D. A., Rozanov, E., Shepherd, T. G., Shibata, K., Tian, W., Braesicke, P., Hardiman, S. C., Lamarque, J. F., Morgenstern, O., Pyle, J. A., Smale, D., and Yamashita, Y.: Multi-model assessment of stratospheric ozone return dates and ozone recovery in CCMVal-2 models, Atmospheric Chemistry and Physics, 10, 9451–9472, doi:10.5194/acp-10-9451-2010, http://www.atmos-chem-phys.net/10/9451/2010/, 2010.

Fiore, A. M., Dentener, F. J., Wild, O., Cuvelier, C., Schultz, M. G., Hess, P., Textor, C., Schulz, M., Doherty, R. M., Horowitz, L. W., MacKenzie, I. A., Sanderson, M. G., Shindell, D. T., Stevenson, D. S., Szopa, S., Van Dingenen, R., Zeng, G., Atherton, C., Bergmann, D., Bey, I., Carmichael, G., Collins, W. J., Duncan, B. N., Faluvegi, G., Folberth, G., Gauss, M., Gong, S., Hauglustaine, D., Holloway, T., Isaksen, I. S. A., Jacob, D. J., Jonson, J. E., Kaminski, J. W., Keating, T. J., Lupu, A., Marmer, E., Montanaro, V., Park, R. J., Pitari, G., Pringle, K. J., Pyle, J. A., Schroeder, S., Vivanco, M. G., Wind, P., Wojcik, G., Wu, S., and Zuber,

A.: Multimodel estimates of intercontinental source-receptor relationships for ozone pollution, J. Geophys. Res., 114, D04301, doi:10.1029/2008JD010816, http://dx.doi.org/10.1029/2008JD010816, 2009.

Fiore, A. M., Naik, V., Spracklen, D. V., Steiner, A., Unger, N., Prather, M., Bergmann, D., Cameron-Smith, P. J., Cionni, I., Collins, W. J., Dalsoren, S., Eyring, V., Folberth, G. A., Ginoux, P., Horowitz, L. W., Josse, B., Lamarque, J.-F., MacKenzie, I. A., Nagashima, T., O'Connor, F. M., Righi, M., Rumbold, S. T., Shindell, D. T., Skeie, R. B., Sudo, K., Szopa, S., Takemura, T., and Zeng, G.: Global air quality and climate, Chem. Soc. Rev., 41, 6663–6683, doi:10.1039/C2CS35095E, http://dx.doi.org/10.1039/C2CS35095E, 2012.

Ganzeveld, L., Bouwman, L., Stehfest, E., van Vuuren, D. P., Eickhout, B., and Lelieveld, J.: Impact of future land use and land cover changes on atmospheric chemistry-climate interactions, J. Geophys. Res., 115, D23301, doi:10.1029/2010JD014041, http://dx.doi.org/10.1029/2010JD014041, 2010.

Ghude, S. D., Jena, C., Chate, D. M., Beig, G., Pfister, G. G., Kumar, R., and Ramanathan, V.: Reductions in India's crop yield due to ozone, Geophysical Research Letters, 41, 5685–5691, doi:10.1002/2014GL060930, http://dx.doi.org/10.1002/2014GL060930, 2014.

Guenther, A. B., Jiang, X., Heald, C. L., Sakulyanontvittaya, T., Duhl, T., Emmons, L. K., and Wang, X.: The Model of Emissions of Gases and Aerosols from Nature version 2.1 (MEGAN2.1): an extended and updated framework for modeling biogenic emissions, Geoscientific Model Development, 5, 1471–1492, doi:10.5194/gmd-5-1471-2012, http://www.geosci-model-dev.net/5/1471/2012/, 2012.

Hand, J. L., Schichtel, B. A., Malm, W. C., and Pitchford, M. L.: Particulate sulfate ion concentration and SO_2 emission trends in the United States from the early 1990s through 2010, Atmospheric Chemistry and Physics, 12, 10 353–10 365, doi:10.5194/acp-12-10353-2012, http://www.atmos-chem-phys.net/12/10353/2012/, 2012.

Heald, C. L., Henze, D. K., Horowitz, L. W., Feddema, J., Lamarque, J.-F., Guenther, A., Hess, P. G., Vitt, F., Seinfeld, J. H., Goldstein, A. H., and Fung, I.: Predicted change in global secondary organic aerosol concentrations in response to future climate, emissions, and land use change, Journal of Geophysical Research: Atmospheres, 113, D05211, doi:10.1029/2007JD009092, http://dx.doi.org/10.1029/2007JD009092, 2008.

Hollaway, M. J., Arnold, S. R., Challinor, A. J., and Emberson, L. D.: Intercontinental trans-boundary contributions to ozone-induced crop yield losses in the Northern Hemisphere, Biogeosciences, 9, 271–292, doi:10.5194/bg-9-271-2012, http://www.biogeosciences.net/9/271/2012/, 2012.

Horowitz, L. W., Fiore, A. M., Milly, G. P., Cohen, R. C., Perring, A., Wooldridge, P. J., Hess, P. G., Emmons, L. K., and Lamarque, J.-F.: Observational constraints on the chemistry of isoprene nitrates over the eastern United States, Journal of Geophysical Research: Atmospheres, 112, D12S08, doi:10.1029/2006JD007747, http://dx.doi.org/10.1029/2006JD007747, 2007.

Hurtt, G., Chini, L., Frolking, S., Betts, R., Feddema, J., Fischer, G., Fisk, J., Hibbard, K., Houghton, R., Janetos, A., Jones, C., Kindermann, G., Kinoshita, T., Klein Goldewijk, K., Riahi, K., Shevliakova, E., Smith, S., Stehfest, E., Thomson, A., Thornton, P., Vuuren, D., and Wang, Y.: Harmonization of land-use scenarios for the period 1500–2100: 600 years of global gridded annual land-use transitions, wood harvest, and resulting secondary lands, Climatic Change, 109, 117–161, doi:10.1007/s10584-011-0153-2, http://dx.doi.org/10.1007/s10584-011-0153-2, 2011.

705 IPCC: in: Climate Change 2013: The Physical Science Basis, edited by Stocker, T., Qin, D., Plattner, G.-K., Tignor, M., Allen, S., Boschung, J., Nauels, A., Y. Xia, V. B., and Midgley, P., p. 1535 pp, Cambridge University Press, Cambridge, United Kingdom and New York, NY, USA, 2013.

Jacob, D. J. and Winner, D. A.: Effect of climate change on air quality, Atmospheric Environment, 43, 51 – 63, doi:http://dx.doi.org/10.1016/j.atmosenv.2008.09.051, http://www.sciencedirect.com/science/article/pii/

710 S1352231008008571, atmospheric Environment - Fifty Years of Endeavour, 2009.

Kawase, H., Nagashima, T., Sudo, K., and Nozawa, T.: Future changes in tropospheric ozone under Representative Concentration Pathways (RCPs), Geophysical Research Letters, 38, L05801, doi:10.1029/2010GL046402, http://dx.doi.org/10.1029/2010GL046402, 2011.

Kaynak, B., Hu, Y., Martin, R. V., Russell, A. G., Choi, Y., and Wang, Y.: The effect of lightning NO_x produc-

715 tion on surface ozone in the continental United States, Atmospheric Chemistry and Physics, 8, 5151–5159, doi:10.5194/acp-8-5151-2008, http://www.atmos-chem-phys.net/8/5151/2008/, 2008.

Kelly, J., Makar, P. A., and Plummer, D. A.: Projections of mid-century summer air-quality for North America: effects of changes in climate and precursor emissions, Atmospheric Chemistry and Physics, 12, 5367–5390, doi:10.5194/acp-12-5367-2012, http://www.atmos-chem-phys.net/12/5367/2012/, 2012.

720 Lack, D. A., Tie, X. X., Bofinger, N. D., Wiegand, A. N., and Madronich, S.: Seasonal variability of secondary organic aerosol: A global modeling study, Journal of Geophysical Research: Atmospheres, 109, D03203, doi:10.1029/2003JD003418, http://dx.doi.org/10.1029/2003JD003418, 2004.

Lam, Y. F., Fu, J. S., Wu, S., and Mickley, L. J.: Impacts of future climate change and effects of biogenic emissions on surface ozone and particulate matter concentrations in the United States, Atmospheric

725 Chemistry and Physics, 11, 4789–4806, doi:10.5194/acp-11-4789-2011, http://www.atmos-chem-phys.net/11/4789/2011/, 2011.

Lamarque, J.-F., Bond, T. C., Eyring, V., Granier, C., Heil, A., Klimont, Z., Lee, D., Liousse, C., Mieville, A., Owen, B., Schultz, M. G., Shindell, D., Smith, S. J., Stehfest, E., Van Aardenne, J., Cooper, O. R., Kainuma, M., Mahowald, N., McConnell, J. R., Naik, V., Riahi, K., and van Vuuren, D. P.: Historical (1850–

730 2000) gridded anthropogenic and biomass burning emissions of reactive gases and aerosols: methodology and application, Atmospheric Chemistry and Physics, 10, 7017–7039, doi:10.5194/acp-10-7017-2010, http://www.atmos-chem-phys.net/10/7017/2010/, 2010.

Lamarque, J.-F., Emmons, L. K., Hess, P. G., Kinnison, D. E., Tilmes, S., Vitt, F., Heald, C. L., Holland, E. A., Lauritzen, P. H., Neu, J., Orlando, J. J., Rasch, P. J., and Tyndall, G. K.: CAM-Chem: description

735 and evaluation of interactive atmospheric chemistry in the Community Earth System Model, Geosci. Model Dev., 5, 369–411, doi:10.5194/gmd-5-369-2012, http://www.geosci-model-dev.net/5/369/2012/, 2012.

Lapina, K., Henze, D. K., Milford, J. B., Huang, M., Lin, M., Fiore, A. M., Carmichael, G., Pfister, G. G., and Bowman, K.: Assessment of source contributions to seasonal vegetative exposure to ozone in the U.S., Journal of Geophysical Research: Atmospheres, 119, 324–340, doi:10.1002/2013JD020905, http://dx.doi.

740 org/10.1002/2013JD020905, 2014.

Lefohn, A. S., Laurence, J. A., and Kohut, R. J.: A comparison of indices that describe the relationship between exposure to ozone and reduction in the yield of agricultural crops, Atmospheric Environment (1967), 22, 1229 – 1240, doi:http://dx.doi.org/10.1016/0004-6981(88)90353-8, http://www.sciencedirect.com/science/article/pii/0004698188903538, 1988.

745 Leibensperger, E. M., Mickley, L. J., Jacob, D. J., Chen, W.-T., Seinfeld, J. H., Nenes, A., Adams, P. J., Streets, D. G., Kumar, N., and Rind, D.: Climatic effects of 1950–2050 changes in US anthropogenic aerosols, Part 1: Aerosol trends and radiative forcing, Atmospheric Chemistry and Physics, 12, 3333–3348, doi:10.5194/acp-12-3333-2012, http://www.atmos-chem-phys.net/12/3333/2012/, 2012.

Leung, L. R. and Gustafson, W. I.: Potential regional climate change and implications to U.S. air qual-
750 ity, Geophysical Research Letters, 32, L16711, doi:10.1029/2005GL022911, http://dx.doi.org/10.1029/2005GL022911, 2005.

Lin, M., Fiore, A. M., Horowitz, L. W., Cooper, O. R., Naik, V., Holloway, J., Johnson, B. J., Middlebrook, A. M., Oltmans, S. J., Pollack, I. B., Ryerson, T. B., Warner, J. X., Wiedinmyer, C., Wilson, J., and Wyman, B.: Transport of Asian ozone pollution into surface air over the western United States in spring, Journal of
755 Geophysical Research: Atmospheres, 117, D00V07, doi:10.1029/2011JD016961, http://dx.doi.org/10.1029/2011JD016961, 2012.

Mahowald, N. M., Lamarque, J.-F., Tie, X. X., and Wolff, E.: Sea-salt aerosol response to climate change: Last Glacial Maximum, preindustrial, and doubled carbon dioxide climates, Journal of Geophysical Research: Atmospheres, 111, D05303, doi:10.1029/2005JD006459, http://dx.doi.org/10.1029/2005JD006459, 2006a.

760 Mahowald, N. M., Muhs, D. R., Levis, S., Rasch, P. J., Yoshioka, M., Zender, C. S., and Luo, C.: Change in atmospheric mineral aerosols in response to climate: Last glacial period, preindustrial, mod-ern, and doubled carbon dioxide climates, Journal of Geophysical Research: Atmospheres, 111, D10202, doi:10.1029/2005JD006653, http://dx.doi.org/10.1029/2005JD006653, 2006b.

Malm, W. C. and Hand, J. L.: An examination of the physical and optical properties of
765 aerosols collected in the {IMPROVE} program, Atmospheric Environment, 41, 3407 – 3427, doi:http://dx.doi.org/10.1016/j.atmosenv.2006.12.012,   http://www.sciencedirect.com/science/article/pii/S1352231006012702, 2007.

Mao, J., Paulot, F., Jacob, D. J., Cohen, R. C., Crounse, J. D., Wennberg, P. O., Keller, C. A., Hudman, R. C., Barkley, M. P., and Horowitz, L. W.: Ozone and organic nitrates over the eastern United States:
770 Sensitivity to isoprene chemistry, Journal of Geophysical Research: Atmospheres, 118, 11,256–11,268, doi:10.1002/jgrd.50817, http://dx.doi.org/10.1002/jgrd.50817, 2013.

Meehl, G. A., Hu, A., Tebaldi, C., Arblaster, J. M., Washington, Warren M.and Teng, H., Sanderson, B. M., Ault, T., Strand, W. G., and White, J. B.: Relative outcomes of climate change mitigation related to temperature versus sea level and sea level rise, Nat. Climate Change, 2, 576–580, doi:10.1038/nclimate1529, 2012.

775 Metzger, S., Dentener, F., Pandis, S., and Lelieveld, J.: Gas/aerosol partitioning: 1. A computation-ally efficient model, Journal of Geophysical Research: Atmospheres, 107, ACH 16–1–ACH 16–24, doi:10.1029/2001JD001102, http://dx.doi.org/10.1029/2001JD001102, 2002.

Moritz, M. A., Parisien, M.-A., Batllori, E., Krawchuk, M. A., Van Dorn, J., Ganz, D. J., and Hayhoe, K.: Climate change and disruptions to global fire activity, Ecosphere, 3, 49, doi:10.1890/ES11-00345.1, http:
780 //dx.doi.org/10.1890/ES11-00345.1, 2012.

Moss, R. H., Edmonds, J. A., Hibbard, K. A., Manning, M. R., Rose, S. K., van Vuuren, D. P., Carter, T. R., Emori, S., Kainuma, M., Kram, T., Meehl, G. A., Mitchell, J. F. B., Nakicenovic, N., Riahi, K., Smith, S. J., Stouffer, R. J., Thomson, A. M., Weyant, J. P., and Wilbanks, T. J.: The next generation of scenarios for climate change and assessment, Nature, 463, 747–756, doi:10.1038/nature08823, 2011.

785 Murazaki, K. and Hess, P.: How does climate change contribute to surface ozone change over the United States?, J. Geophys. Res., 111, D05301, doi:10.1029/2005JD005873, http://dx.doi.org/10.1029/2005JD005873, 2006.

Neale, R. B., Richter, J., Park, S., Lauritzen, P. H., Vavrus, S. J., Rasch, P. J., and Zhang, M.: The mean climate of the community atmosphere model (CAM4) in forced SST and fully coupled experiments., J. Climate, 26,

790 5150–5168, doi:http://dx.doi.org/10.1175/JCLI-D-12-00236, 2013.

Nolte, C. G., Gilliland, A. B., Hogrefe, C., and Mickley, L. J.: Linking global to regional models to assess future climate impacts on surface ozone levels in the United States, Journal of Geophysical Research: Atmospheres, 113, D14307, doi:10.1029/2007JD008497, http://dx.doi.org/10.1029/2007JD008497, 2008.

Oleson, K. W., Lawrence, D. M., Bonan, G. B., Flanner, M. G., Kluzek, E., Lawrence, P. J., Levis, S., Swenson,

795 S. C., Thornton, P. E., Dai, A., M., D., Dickinson, R., Feddema, J., Heald, C. L., Hoffman, F., Lamarque, J.-F., Mahowald, N., Niu, G.-Y., Qian, T., Randerson, J., Running, S., Sakaguchi, K., Slater, A., Stockli, R., Wang, A., Yang, Z.-L., and Zeng, X.: Technical description of version 4.0 of the Community Land Model (CLM), Tech. Rep. Technical Note NCAR/TN-478+STR, 257 pp., NCAR, 2010.

Parrish, D. D., Lamarque, J.-F., Naik, V., Horowitz, L., Shindell, D. T., Staehelin, J., Derwent, R., Cooper,

800 O. R., Tanimoto, H., Volz-Thomas, A., Gilge, S., Scheel, H.-E., Steinbacher, M., and Fröhlich, M.: Long-term changes in lower tropospheric baseline ozone concentrations: Comparing chemistry-climate models and observations at northern midlatitudes, Journal of Geophysical Research: Atmospheres, 119, 5719–5736, doi:10.1002/2013JD021435, http://dx.doi.org/10.1002/2013JD021435, 2014.

Pfister, G. G., Walters, S., Lamarque, J.-F., Fast, J., Barth, M. C., Wong, J., Done, J., Holland, G., and Brussere,

805 C. L.: Projections of future summertime ozone over the U.S., Journal of Geophysical Research: Atmospheres, 119, 5559–5582, doi:10.1002/2013JD020932, http://dx.doi.org/10.1002/2013JD020932, 2014.

Pitchford, M. L. and Malm, W. C.: Development and applications of a standard visual index, Atmospheric Environment, 28, 1049 – 1054, doi:http://dx.doi.org/10.1016/1352-2310(94)90264-X, http://www.sciencedirect.com/science/article/pii/135223109490264X, conference on visibility and fine particles, 1994.

810 Pope, C. A. and Dockery, D. W.: Health Effects of Fine Particulate Air Pollution: Lines that Connect, Journal of the Air and Waste Management Association, 56, 709–742, doi:10.1080/10473289.2006.10464485, 2006.

Pye, H. O. T., Liao, H., Wu, S., Mickley, L. J., Jacob, D. J., Henze, D. K., and Seinfeld, J. H.: Effect of changes in climate and emissions on future sulfate-nitrate-ammonium aerosol levels in the United States, Journal of Geophysical Research: Atmospheres, 114, D01205, doi:10.1029/2008JD010701, http://dx.doi.org/10.1029/

815 2008JD010701, 2009.

Racherla, P. N. and Adams, P. J.: The response of surface ozone to climate change over the Eastern United States, Atmospheric Chemistry and Physics, 8, 871–885, doi:10.5194/acp-8-871-2008, http://www.atmos-chem-phys.net/8/871/2008/, 2008.

Reich, P. B. and Amundson, R. G.: Ambient levels of ozone reduce net photosynthesis in tree and crop species,

820 Science, 230, 566–570, doi:10.1126/science.230.4725.566, 1985.

Schaub, M., J., Skelly, J., Zhang, J., Ferdinand, J., Savage, J., Stevenson, R., Davis, D., and Steiner, K.: Physiological and foliar symptom response in the crowns of Prunus serotina, Fraxinus americana and Acer rubrum canopy trees to ambient ozone under forest conditions, Science, 133, 553–567, doi:10.1016/j.envpol.2004.06.012, 2005.

825 Scholze, M., Knorr, W., Arnell, N. W., and Prentice, I. C.: A climate-change risk analysis for world ecosystems, Proceedings of the National Academy of Sciences, 103, 13 116–13 120, doi:10.1073/pnas.0601816103, http://www.pnas.org/content/103/35/13116.abstract, 2006.

Sitch, S., Cox, P. M., Collins, W. J., and Huntingford, C.: Indirect radiative forcing of climate change through ozone effects on the land-carbon sink, Nature, 448, 791–794, doi:10.1038/nature06059, 2007.

830 Spracklen, D. V., Mickley, L. J., Logan., J. A., Hudman, R. C., Yevich, R., Flannigan, M. D., and Westerling, A. L.: Impacts of climate change from 2000 to 2050 on wildfire activity and carbonaceous aerosol concentrations in the western United States, J. Geophys. Res., 114, D2030, doi:10.1029/2008JD010966, 2009.

Tagaris, E., Manomaiphiboon, K., Liao, K.-J., Leung, L. R., Woo, J.-H., He, S., Amar, P., and Russell, A. G.: Impacts of global climate change and emissions on regional ozone and fine particulate mat-

835 ter concentrations over the United States, Journal of Geophysical Research: Atmospheres, 112, D14312, doi:10.1029/2006JD008262, http://dx.doi.org/10.1029/2006JD008262, 2007.

Tai, A. P. K., Mickley, L. J., and Jacob, D. J.: Impact of 2000–2050 climate change on fine particulate matter ($PM_{2.5}$) air quality inferred from a multi-model analysis of meteorological modes, Atmospheric Chemistry and Physics, 12, 11 329–11 337, doi:10.5194/acp-12-11329-2012, http://www.atmos-chem-phys.net/

840 12/11329/2012/, 2012.

Tai, A. P. K., Mickley, L. J., Heald, C. L., and Wu, S.: Effect of CO2 inhibition on biogenic isoprene emission: Implications for air quality under 2000 to 2050 changes in climate, vegetation, and land use, Geophysical Research Letters, 40, 3479–3483, doi:10.1002/grl.50650, http://dx.doi.org/10.1002/grl.50650, 2013.

Tai, A. P. K., Val Martin, M., and Heald, C. L.: Threat to future global food security from climate change and

845 ozone air pollution, Nature Climate Change, 4, 817–821, doi:10.1038/nclimate2317, 2014.

Tie, X., Madronich, S., Walters, S., Edwards, D. P., Ginoux, P., Mahowald, N., Zhang, R., Lou, C., and Brasseur, G.: Assessment of the global impact of aerosols on tropospheric oxidants, Journal of Geophysical Research: Atmospheres, 110, D03204, doi:10.1029/2004JD005359, http://dx.doi.org/10.1029/2004JD005359, 2005.

Tilmes, S., Lamarque, J.-F., Emmons, L. K., Kinnison, D. E., Ma, P.-L., Liu, X., Ghan, S., Bardeen, C.,

850 Arnold, S., Deeter, M., Vitt, F., Ryerson, T., Elkins, J. W., Moore, F., and Spackman, R.: Description and evaluation of tropospheric chemistry and aerosols in the Community Earth System Model (CESM1.2), Geoscientific Model Development Discussions, 7, 8875–8940, doi:10.5194/gmdd-7-8875-2014, http://www.geosci-model-dev-discuss.net/7/8875/2014/, 2014.

Tong, D. Q., Mathur, R., Kang, D., Yu, S., Schere, K. L., and Pouliot, G.: Vegetation exposure to ozone

855 over the continental United States: Assessment of exposure indices by the Eta-CMAQ air quality forecast model, Atmospheric Environment, 43, 724 – 733, doi:http://dx.doi.org/10.1016/j.atmosenv.2008.09.084, http://www.sciencedirect.com/science/article/pii/S1352231008009047, 2009.

US EPA: Guidance for Estimating Natural Visibility Conditions Under the Regional Haze Rule, Tech. Rep. EPA 454/B-03-005, U.S. Environmental Protection Agency Office of Air Quality Planning and Standards

860 Emissions, Monitoring and Analysis Division Air Quality Trends Analysis Group, Research Triangle Park, NC, 2003.

Val Martin, M., Heald, C. L., Ford, B., Prenni, A. J., and Wiedinmyer, C.: A decadal satellite analysis of the origins and impacts of smoke in Colorado, Atmospheric Chemistry and Physics, 13, 7429–7439, doi:10.5194/acp-13-7429-2013, http://www.atmos-chem-phys.net/13/7429/2013/, 2013.

24

Table 1. Summary of main RCP4.5 and RCP8.5 anthropogenic greenhouse gas concentrations and global area-averaged sea-surface temperature (SST) for 2000 and 2050.

Year	Scenario	CO_2 (ppm)	CH_4 (ppb)	N_2O (ppb)	SST (°C)
2000	Baseline	367	1760	316	12.2
2050	RCP4.5	487	1833	350	12.6
	RCP8.5	541	2740	367	13.0

865   Val Martin, M., Heald, C. L., and Arnold, S. R.: Coupling dry deposition to vegetation phenology in the Community Earth System Model: Implications for the simulation of surface O_3, Geophysical Research Letters, 41, 2988–2996, doi:10.1002/2014GL059651, http://dx.doi.org/10.1002/2014GL059651, 2014.

van Vuuren, D., Edmonds, J., Kainuma, M., Riahi, K., Thomson, A., Hibbard, K., Hurtt, G., Kram, T., Krey, V., Lamarque, J.-F., Masui, T., Meinshausen, M., Nakicenovic, N., Smith, S., and Rose, S.: The representative

870   concentration pathways: an overview, Climatic Change, 109, 5–31, doi:10.1007/s10584-011-0148-z, http://dx.doi.org/10.1007/s10584-011-0148-z, 2011.

Wesely, M.: Parameterization of surface resistances to gaseous dry deposition in regional-scale numerical models, Atmos. Environ., 23, 1293–1304, doi:http://dx.doi.org/10.1016/0004-6981(89)90153-4, http://www.sciencedirect.com/science/article/pii/0004698189901534, 1989.

875   Wu, S., Mickley, L. J., Jacob, D. J., Rind, D., and Streets, D. G.: Effects of 2000–2050 changes in climate and emissions on global tropospheric ozone and the policy-relevant background surface ozone in the United States, Journal of Geophysical Research: Atmospheres, 113, D18312, doi:10.1029/2007JD009639, http://dx.doi.org/10.1029/2007JD009639, 2008.

Wu, S., Mickley, L. J., Kaplan, J. O., and Jacob, D. J.: Impacts of changes in land use and land cover

880   on atmospheric chemistry and air quality over the 21st century, Atmos. Chem. Phys., 12, 1597–1609, doi:10.5194/acp-12-1597-2012, http://www.atmos-chem-phys.net/12/1597/2012/, 2012.

Yue, X., Mickley, L. J., Logan, J. A., and Kaplan, J. O.: Ensemble projections of wildfire activity and carbonaceous aerosol concentrations over the western United States in the mid-21st century, Atmospheric Environment, 77, 767 – 780, doi:http://dx.doi.org/10.1016/j.atmosenv.2013.06.003, http://www.sciencedirect.com/

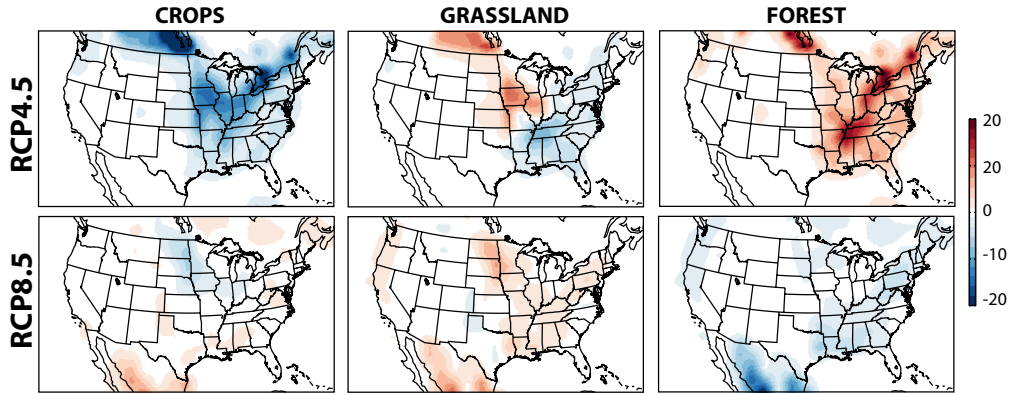885   science/article/pii/S1352231013004573, 2013.

Figure 1. Projected 2050-2000 changes (%) in forest, grasslands and croplands by the RCP4.5 and RCP8.5 scenarios.
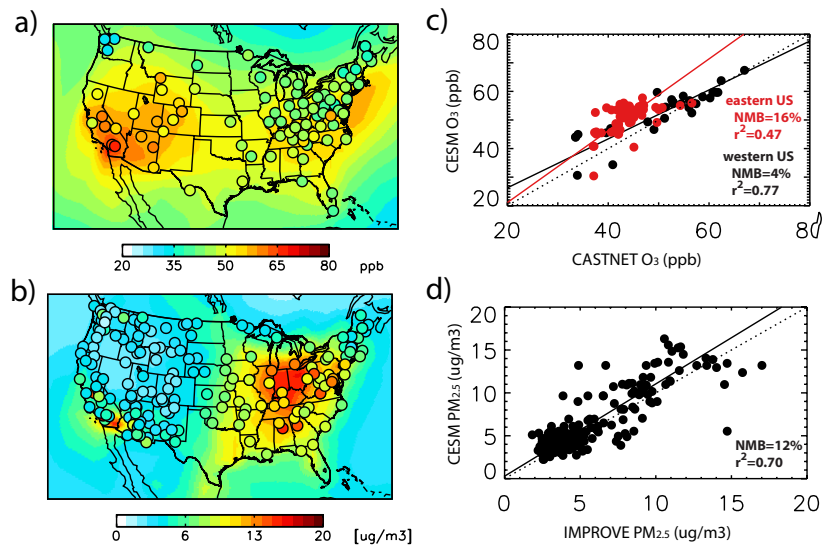

Figure 2. Simulated and observed present-day surface MDA-8 O_3 and $PM_{2.5}$ (a,b) and the scatter plots with modeled and observed values at the individual sites (c,d). Observations are long-term means from the CAST-NET (1995–2005) and IMPROVE (1998–2010) networks. The squared-correlation coefficients (r^2) and normalized mean biases (NMB) are shown in the inset. Reduced-major axis regression lines (solid) and the 1:1 lines (dash) are also shown. Maps show interpolated contours from the 1.9x2.5 degree horizontal resolution output.
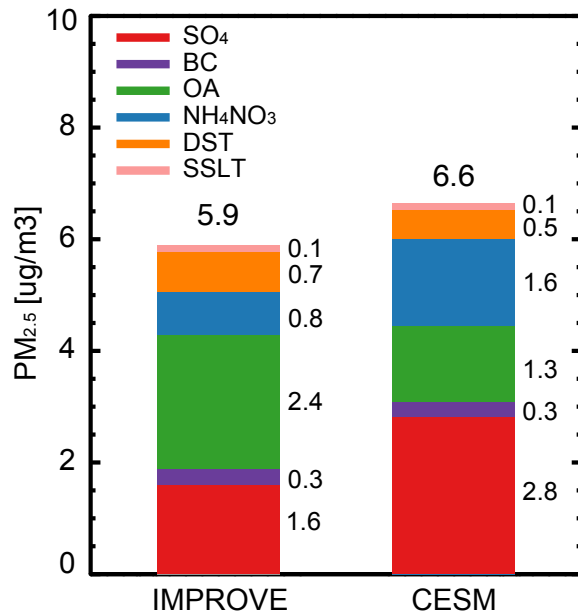
Figure 3. Simulated and observed $PM_{2.5}$ chemical species over the United States. Big numerals indicate the annual $PM_{2.5}$ concentrations, whereas small numerals indicate $PM_{2.5}$ chemical species concentrations.
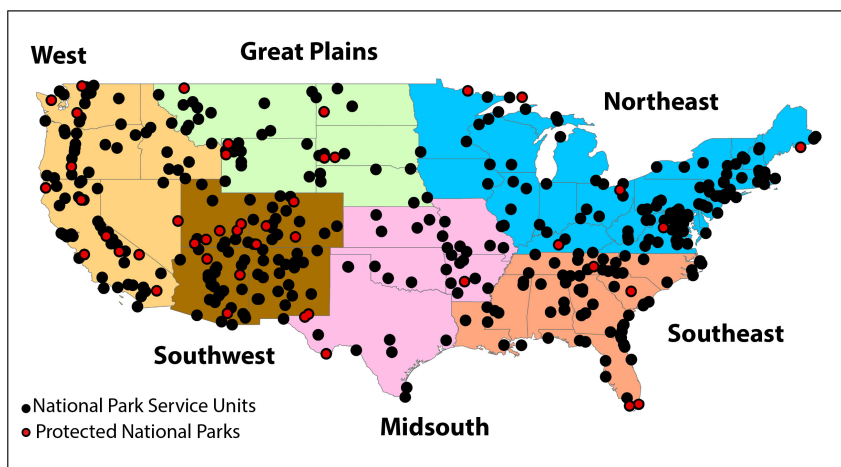

Figure 4. Location of the U.S. National Park units and wilderness areas used in this study. The U.S. protected National Parks are highlighted in red; the six U.S. climatic regions are also identified.
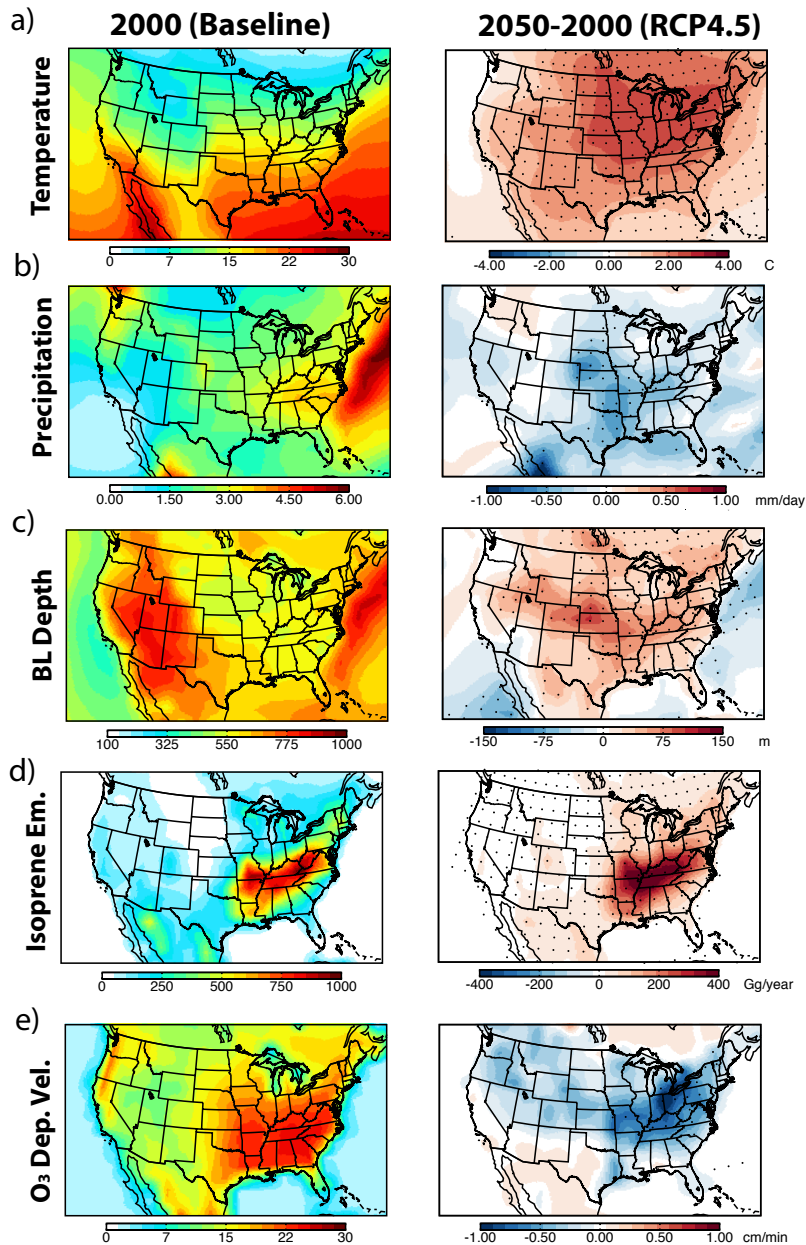
Figure 5. Simulated annual average present-day (left) and projected 2050–2000 changes (right) for surface temperature (a), precipitation (b), boundary layer depth (c), isoprene emissions (d) and O_3 dry deposition velocity (e). All maps show changes predicted by the RCP4.5 as a result of the combination of climate, land use and emissions changes, except for the O_3 dry deposition velocity that shows only the changes from land use. Regions with changes that are significant at the 95% confidence level are indicated in the maps with dots, and maps show interpolated contours from the 1.9x2.5 degree horizontal resolution output.

Table 2. Anthropogenic short-lived air pollutants and biogenic emissions in 2000 and 2050, projected by the RCP4.5 and RCP8.5 scenarios over the United States.

Year	Scenario	Anthropogenic Emissions[a]							Biogenic Emissions[b]	
		BC	OC	CO	NO_x	NH_3	NMVOCs	SO_2	Isoprene	Monoterpenes
					eastern U.S.					
2000	Baseline	0.29	0.41	70.38	4.82	1.53	1.96	6.30	20.5	6.3
2050	RCP4.5	0.15	0.19	8.70	1.04	1.92	0.90	0.80	33.7	9.4
2050	RCP8.5	0.03	0.06	7.99	1.35	2.21	0.36	0.63	27.8	8.0
					western U.S.					
2000	Baseline	0.10	0.15	25.82	1.58	1.36	0.64	1.77	7.4	2.5
2050	RCP4.5	0.05	0.08	3.55	0.39	1.81	0.30	0.29	9.4	3.0
2050	RCP8.5	0.02	0.03	7.20	0.79	2.16	0.15	0.54	9.6	3.3

[a] Reported Tg C/year for BC, OC and NMVOCs; Tg N/year for NO_x and NH_3; Tg S/year for SO_2; and Tg CO/year for CO.
[b] Reported Tg C/year.

Table 3. List of simulations[a]

Forcings	2000 Baseline	2050 Total	2050 Climate	2050 Emissions	2050 Land Use
Climate	2000	2050	2050	2000	2000
Emissions[b]:					
Anthropogenic	2000	2050	2000	2050	2000
BB	2000	2050	2000	2050	2000
Biogenic	2000	2050	2000	2000	2050
Land Use[c]	2000	2050	2000	2000	2050
Methane	2000	2050	2000	2050	2000

[a] Years represent the year forcing parameter selected for each simulation.
[b] Anthropogenic is the RCP surface and ship emissions, BB is the RCP biomass burning emissions and are considered anthropogenic impact; Biogenic is biogenic emissions calculated by MEGAN v2.1 (see text for further explanation).
[c] Land is the human induced land cover and land use projected by the RCP scenarios.

Table 4. Simulated annual air quality over the U.S. National Parks and wilderness areas[a]

National Park	$PM_{2.5}$ ($\mu g/m^3$) 2000 Base	2050 RCP4.5	2050 RCP8.5	MDA-8 O_3 (ppb) 2000 Base	2050 RCP4.5	2050 RCP8.5	W126 O_3 (ppm-hr) 2000 Base	2050 RCP4.5	2050 RCP8.5
Acadia, ME (44° N, 68° W)	4.3	2.2	2.2	48.0	43.9	48.8	13.1	2.5	4.7
Arches, UT (39° N, 110° W)	3.2	1.6	2.6	57.8	51.2	60.8	39.9	10.4	39.1
Badlands, SD (44° N, 102° W)	4.1	1.7	3.1	49.4	47.8	55.1	15.9	11.5	29.2
Big Bend, TX (29° N, 103° W)	5.2	2.9	3.8	47.0	42.9	49.4	5.9	2.9	8.5
Biscayne, FL (26° N, 80° W)	5.9	3.9	3.3	45.7	40.4	45.6	1.1	0.5	1.0
Black Canyon, CO (39° N, 108° W)	3.3	1.8	2.8	57.0	50.9	60.4	34.5	8.7	34.6
Bryce Canyon, UT (38° N, 112° W)	4.1	2.1	3.2	58.7	51.7	59.7	45.8	12.1	33.3
Canyonlands, UT (38° N, 110° W)	3.2	1.6	2.6	57.8	51.2	60.8	39.9	10.4	39.1
Capitol Reef, UT (38° N, 111° W)	3.2	1.6	2.6	57.8	51.2	60.8	39.9	10.4	39.1
Carlsbad Caverns, NM (32° N, 104° W)	5.0	2.6	3.2	50.7	45.5	52.3	13.4	4.9	13.1
Channel Islands, CA (34° N, 119° W)	8.6	6.2	5.6	52.4	50.2	55.5	12.2	4.6	9.6
Congaree, SC (34° N, 81° W)	10.2	4.6	4.7	53.6	46.3	52.3	23.4	4.2	11.8
Crater Lake, OR (43° N, 122° W)	4.2	4.2	3.0	50.1	46.6	52.2	11.9	3.1	5.4
Cuyahoga Valley, OH (41° N, 82° W)	15.9	5.8	5.2	53.2	49.0	52.3	61.3	21.7	28.4
Death Valley, CA (36° N, 117° W)	3.4	2.1	2.1	58.9	52.7	58.9	45.5	15.1	28.3
Dry Tortugas, FL (25N,83W)	6.0	4.2	4.0	40.8	38.4	44.6	0.6	0.5	1.2
Everglades, FL (25° N, 81° W)	5.9	3.9	3.3	45.7	40.4	45.6	1.1	0.5	1.0
Glacier, MT (49° N, 114° W)	3.1	2.6	2.5	48.5	46.8	52.7	9.5	4.2	9.7
Grand Canyon, AZ (36° N, 113° W)	4.1	2.1	3.2	58.7	51.7	59.7	45.8	12.1	33.3
Grand Teton, WY (44° N, 111° W)	2.2	1.4	1.8	53.8	50.8	58.2	18.1	8.3	22.8
Great Basin, NV (39° N, 114° W)	2.5	1.5	1.7	57.0	51.6	59.0	34.7	11.5	28.2
Great Sand Dunes, CO (38° N, 105° W)	4.2	2.0	3.3	55.9	49.7	59.1	29.7	8.5	32.1
Great Smoky Mountains, NC, TN (36° N, 83° W)	10.9	5.6	4.2	55.7	46.4	51.8	43.8	5.7	14.9
Guadalupe Mountains, TX (32° N, 105° W)	5.0	2.6	3.2	50.7	45.5	52.3	13.4	4.9	13.1
Hot Springs, AR (34° N, 93° W)	10.8	4.7	5.5	53.0	43.9	51.0	32.0	3.9	13.3
Isle Royale, MI (48° N, 88° W)	3.7	2.6	3.0	43.3	42.8	47.7	4.8	2.8	6.5
Joshua Tree, CA (34° N, 116° W)	16.9	13.4	13.9	62.3	53.7	58.4	57.9	20.2	28.2
Kings Canyon, CA (37° N, 118° W)	3.4	2.1	2.1	58.9	52.7	58.9	45.5	15.1	28.3
Lassen Volcanic, CA (40° N, 121° W)	4.7	5.2	3.6	51.2	48.0	54.4	14.0	4.0	9.3
Mammoth Cave, KY (37° N, 86° W)	15.1	6.4	6.2	54.5	46.4	52.4	49.1	7.6	22.6
Mesa Verde, CO (37° N, 108° W)	4.6	2.1	3.9	57.8	50.5	60.6	40.8	8.8	38.6
Mount Rainier, WA (47° N, 122° W)	5.1	3.4	2.6	45.9	43.4	47.8	5.2	1.0	1.6
North Cascades, WA (49° N, 121° W)	4.9	3.2	2.4	45.2	43.3	47.7	6.3	1.2	1.9
Olympic, WA (48° N, 123° W)	4.9	3.2	2.4	45.2	43.3	47.7	6.3	1.2	1.9
Petrified Forest, AZ (35° N, 110° W)	5.5	2.6	4.4	58.2	50.3	59.3	44.0	10.2	34.6
Redwood, CA (41° N, 124° W)	3.4	3.4	2.6	44.9	44.4	49.5	1.2	0.8	1.4
Rocky Mountain, CO (40° N, 106° W)	4.6	2.0	3.1	56.8	51.8	60.0	37.9	13.6	36.4
Saguaro, AZ (32° N, 110° W)	6.1	3.3	4.3	57.8	49.6	56.3	45.0	10.0	23.0
Sequoia, CA (36° N, 119° W)	3.4	2.1	2.1	58.9	52.7	58.9	45.5	15.1	28.3
Shenandoah, VA (38° N, 78° W)	13.2	6.2	4.0	57.0	49.0	51.7	66.5	11.7	13.3
Theodore Roosevelt, ND (47° N, 103° W)	4.8	1.8	3.6	47.8	46.8	53.6	16.2	11.0	29.3
Voyageurs, MN (48° N, 93° W)	4.1	2.3	3.2	43.5	42.9	48.0	5.7	3.0	7.4
Wind Cave, SD (44° N, 103° W)	4.1	1.7	3.1	49.4	47.8	55.1	15.9	11.5	29.2
Yellowstone, WY, MT, ID (45° N, 110° W)	2.2	1.4	1.8	53.8	50.8	58.2	18.1	8.3	22.8
Yosemite, CA (38° N, 119° W)	5.5	3.3	2.7	60.1	52.8	58.5	60.4	18.9	29.1
Zion, UT (37° N, 113° W)	4.1	2.1	3.2	58.7	51.7	59.7	45.8	12.1	33.3

[a] Shown only results for the 46 protected National Parks located in the continental United States; Results from other NPs and wilderness areas can be provided by request.
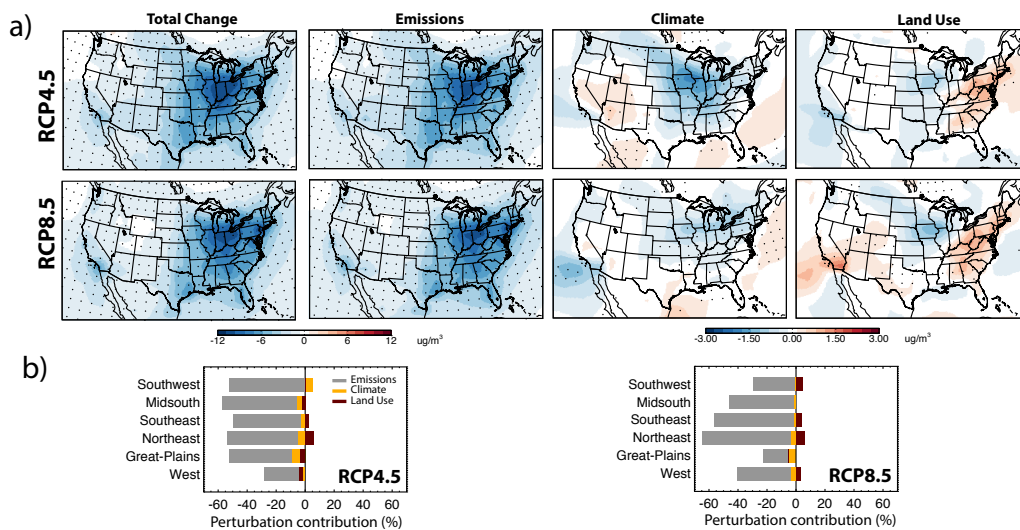
Figure 6. Projected simulated 2050–2000 changes in annual PM$_{2.5}$ as a result of the combination of climate, land use and emissions changes, and the individual changes (a), and the percentage contribution of the individual perturbation (b) for the RCP4.5 and RCP8.5 scenarios. Regions with changes that are significant at the 95% confidence level are indicated in the maps with dots, and maps show interpolated contours from the 1.9x2.5 degree horizontal resolution output. Bars represent the changes (in %) for each individual forcing, i.e., emissions and methane levels (grey), climate (yellow) and land use (dark red).
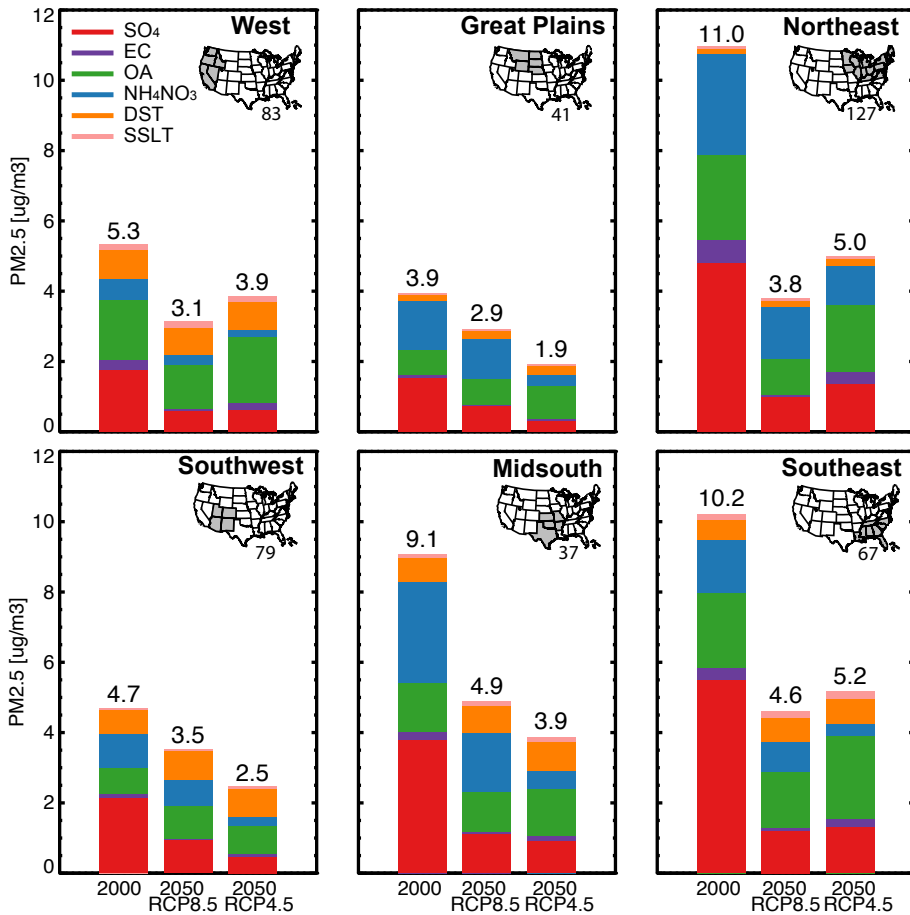
Figure 7. Annual $PM_{2.5}$ chemical species for present-day and 2050 as predicted by the RCP4.5 and RCP8.5 scenarios in the U.S. climatic regions. The inset maps show the states in the region in gray, and the numerals indicate the numbers of U.S. National Parks and wilderness areas in each climatic region. Big numerals indicate the annual $PM_{2.5}$ concentrations.
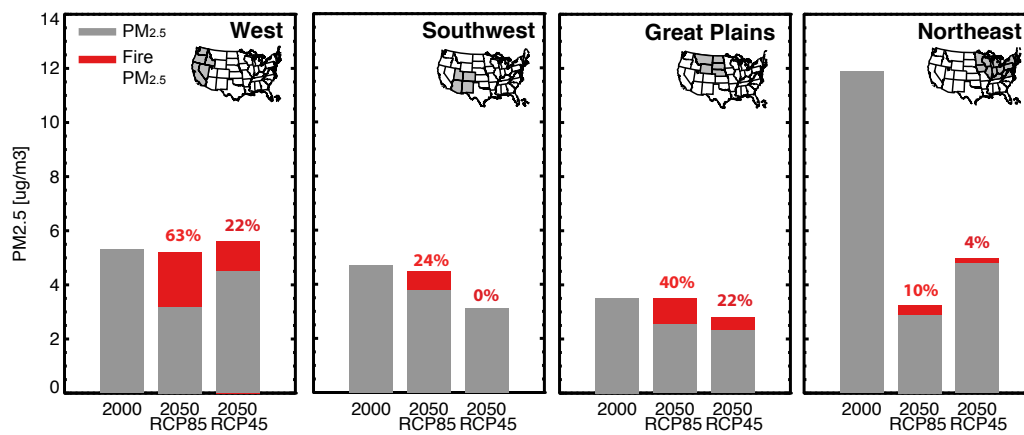
Figure 8. Changes in PM$_{2.5}$ resulting from climate-driven fire activity in the U.S. regions affected by fire. Simulated PM$_{2.5}$ by the RCP scenarios is shown in gray and future PM$_{2.5}$ from climate-driven fire emissions in red. The inset maps show the states in the region in gray and the red numerals indicate the percentage change in PM$_{2.5}$ when climate-driven fire activity is included in the simulation.
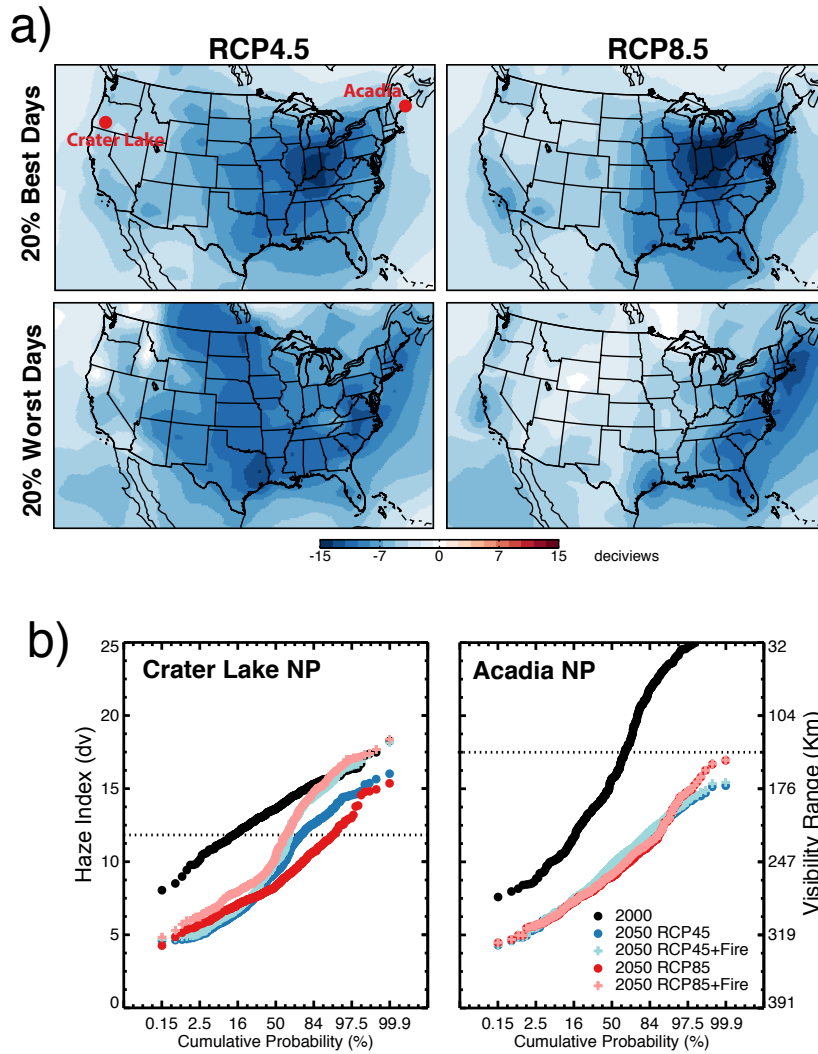
Figure 9. Projected simulated 2050–2000 changes in haze index (HI) as a result of the combination of climate, land use and emissions changes (a) and the cumulative probability distributions of daily mean haze index in the Crater Lake and Acadia NPs (b). Maps show "20% Best Days" as the averaged HI during the cleanest days and "20% Worst Days" as averaged HI during the haziest days (see text for further explanation); data are shown as interpolated contours from the 1.9°x2.5° horizontal resolution output. The location of the Crater Lake and Acadia NPs are indicated in the top left map. The cumulative distribution plots show simulated daily HI for present-day (black circles), 2050 projected by RCP4.5 (blue circles) and by RCP8.5 (red circles), and 2050 with the effects of climate-driven fires by RCP4.5 (light blue cross) and by RCP8.5 (light red cross). The 2050 HI target to reach natural visibility conditions by 2064 are indicated with a horizontal dotted line.
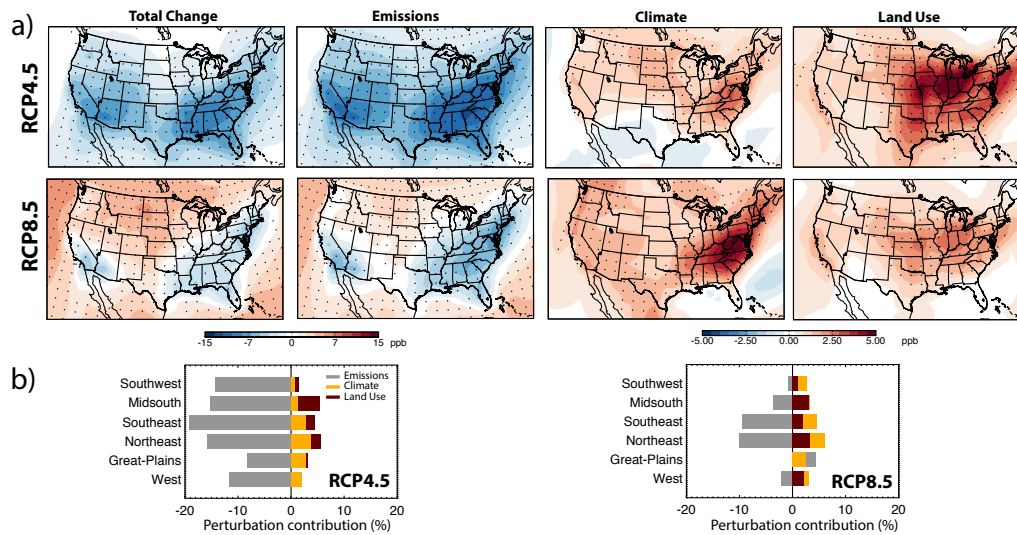
Figure 10. Projected simulated 2050–2000 changes in surface O_3 as a result of the combination of climate, land use and emissions changes, and the individual changes (a) and the percentage contribution of the individual perturbations (b) for the RCP4.5 and RCP8.5 scenarios. Maps show interpolated contours from the 1.9x2.5 degree horizontal resolution output. Regions with changes that are significant at the 95% confidence level are indicated in the maps with dots, and O_3 concentrations are annual maximum daily 8-hour (MDA-8) averages. Bars represent the changes (in %) for each individual forcing, i.e., emissions and methane levels (grey), climate (yellow) and land use (dark red).
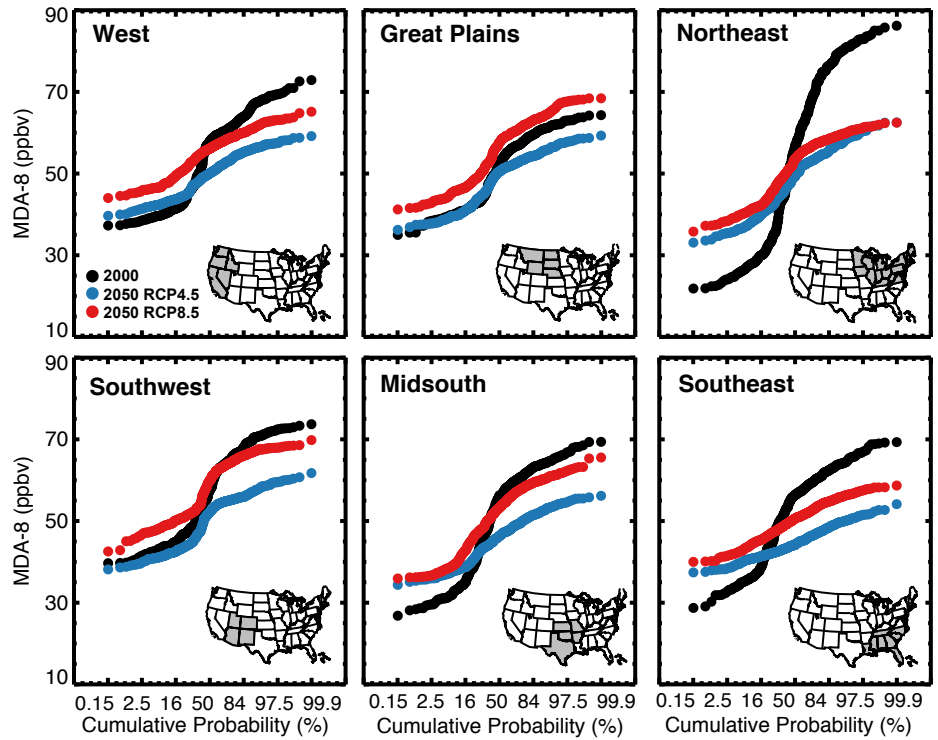
Figure 11. Cumulative probability distributions of simulated surface O_3 MDA-8 averaged over the U.S. National Parks and wilderness areas in the U.S. climatic regions, for present-day (black circles) and 2050 predicted by the RCP4.5 (blue circles) and RCP8.5 (red circles) scenarios. The inset maps show the states in the region in gray.
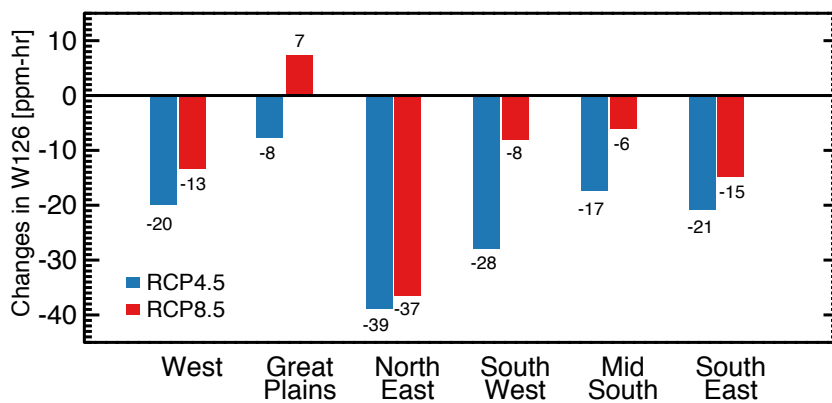

Figure 12. Simulated 2050–2000 summertime changes in O_3 W126 for RCP4.5 (blue) and RCP8.5 (red) averaged over the six U.S. climatic regions identified in Figure 4. Numerals indicate the simulated changes in O_3 W126 (ppm-hr).